Recent changes in terrestrial water storage in the Upper Nile Basin: an evaluation of commonly used gridded GRACE products

Mohammad Shamsudduha[1, 2], Richard G. Taylor[2], Darren Jones[3], Laurent Longuevergne[4], Michael Owor[5] and Callist Tindimugaya[6]

[1]Institute for Risk and Disaster Reduction, University College London, UK
[2]Department of Geography, University College London, UK
[3]Centre for Geography, Environment and Society, University of Exeter, UK
[4]CNRS – UMR 6118 Géosciences Rennes, Université de Rennes 1, France
[5]Department of Geology & Petroleum Studies, Makerere University, Uganda
[6]Directorate of Water Resources Management, Ministry of Water & Environment, Uganda

Correspondence to: M. Shamsudduha (m.shamsudduha@ucl.ac.uk)

Abstract

GRACE (Gravity Recovery and Climate Experiment) satellite data monitor large-scale changes in total terrestrial water storage (ΔTWS) providing an invaluable tool where in situ observations are limited. Substantial uncertainty remains, however, in the amplitude of GRACE gravity signals and the disaggregation of TWS into individual terrestrial water stores (e.g. groundwater storage). Here, we test the phase and amplitude of three GRACE ΔTWS signals from 5 commonly-used gridded products (i.e., NASA's *GRCTellus*: CSR, JPL GFZ; JPL-Mascons; GRGS GRACE) using in situ data and modelled soil-moisture from the Global Land Data Assimilation System (GLDAS) in two sub basins (LVB: Lake Victoria Basin, LKB: Lake Kyoga Basin) of the Upper Nile Basin. The analysis extends from January 2003 to December 2012 but focuses on a large and accurately observed reduction in ΔTWS of 83 km^3 from 2003 to 2006 in Lake Victoria Basin. We reveal substantial variability in current GRACE products to quantify the reduction of ΔTWS in Lake Victoria that ranges from 80 km^3 (JPL-Mascons) to 69 km^3 and 31 km^3 for GRGS and *GRCTellus*, respectively.

Representation of the phase in TWS in the Upper Nile Basin by GRACE products varies but is generally robust with GRGS, JPL-Mascons and *GRCTellus* (ensemble mean of CSR, JPL and GFZ time-series data) explaining 90 %, 84 %, and 75 % of the variance, respectively, in 'in-situ' or 'bottom-up' ΔTWS in LVB. Resolution of changes in groundwater storage (ΔGWS) from GRACE ΔTWS is greatly constrained by both uncertainty in changes in soil-moisture storage (ΔSMS) modelled by GLDAS LSMs (CLM, NOAH, VIC) and the low annual amplitudes in ΔGWS (e.g., 1.8 to 4.9 cm) observed in deeply weathered crystalline rocks underlying the Upper Nile Basin. Our study highlights the substantial uncertainty in the amplitude of ΔTWS that can result from different data-processing strategies in commonly used, gridded GRACE products.

Keywords: GRACE products; terrestrial water storage; groundwater; hard-rock aquifers; Lake Victoria; Lake Kyoga; Sub-Saharan Africa

1. Introduction

Satellite measurements under the Gravity Recovery and Climate Experiment (GRACE) mission have, since March 2002 (Tapley et al., 2004), enabled remote monitoring of large-scale (i.e., GRACE footprint: ~200 000 km^2), spatio-temporal changes in total terrestrial water storage (ΔTWS) at 10-day to monthly timescales (Longuevergne et al., 2013; Humphrey et al., 2016). Over the last 15 years, studies in basins around the world (Rodell and Famiglietti, 2001; Strassberg et al., 2007; Leblanc et al., 2009; Chen et al., 2010; Longuevergne et al., 2010; Frappart et al., 2011; Jacob et al., 2012; Shamsudduha et al., 2012; Arendt et al., 2013; Kusche et al., 2016) have demonstrated that GRACE satellites trace natural (e.g., drought, floods, glaciers and ice melting, sea-level rise) and anthropogenic (e.g., abstraction-driven groundwater depletion) influences on ΔTWS. GRACE-derived TWS

provides vertically-integrated water storage changes in all water-bearing layers (Wahr et al., 2004; Strassberg et al., 2007; Ramillien et al., 2008) that include (Eq. 1) surface water storage in rivers, lakes, and wetlands (ΔSWS), soil moisture storage (ΔSMS), ice and snow water storage (ΔISS), and groundwater storage (ΔGWS). GRACE measurements have over the last decade become an important hydrological tool for quantifying basin-scale ΔTWS (Güntner, 2008; Xie et al., 2012; Hu and Jiao, 2015) and are increasingly being used to assess spatio-temporal changes in specific water stores (Famiglietti et al., 2011; Shamsudduha et al., 2012; Jiang et al., 2014; Castellazzi et al., 2016; Long et al., 2016; Nanteza et al., 2016) where time-series records of other individual freshwater stores are available (Eq. 1).

$$\Delta TWS_t = \Delta GWS_t + \Delta ISS_t + \Delta SWS_t + \Delta SMS_t \quad (1)$$

GRACE-derived ΔTWS derive from monthly gravitational fields which can be represented as spherical harmonic coefficients that are noisy as depicted in north-south elongated linear features or "stripes" on monthly global gravity maps (Swenson and Wahr, 2006; Wang et al., 2016). Post-processing of GRACE SH data is therefore required. The most popular GRACE products are NASA's *GRCTellus* land gravity solutions (i.e., spherical harmonics based CSR, JPL and GFZ), which require scaling factors to recover spatially smoothed TWS signals (Swenson and Wahr, 2006; Landerer and Swenson, 2012). Additionally, NASA's new monthly gridded GRACE product, Mass Concentration blocks (i.e., Mascons), estimate terrestrial mass changes directly from inter-satellite acceleration measurements and can be used without further post-processing (Rowlands et al., 2010; Watkins et al., 2015). GRGS GRACE are also spherical harmonic-based products available at a 10-day timestep and can also be used directly since gravity fields are stabilised during the processing of GRACE satellite data (Lemoine et al., 2007; Bruinsma et al., 2010).

Restoration of the amplitude of *GRCTellus* TWS data, dampened by spatial Gaussian filtering with a large smoothing radius (e.g., 300 to 500 km), is commonly achieved using scaling factors that derive from a priori model of freshwater stores, usually a global-scale Land-Surface Model or LSM (Long et al., 2015). However, signal-restoration methods are emerging that do not require hydrological model or LSM (Vishwakarma et al., 2016). Substantial uncertainty nevertheless persists in the magnitude of applied scaling factors (e.g., *GRCTellus*) and corrections (Long et al., 2015). In situ observations provide a valuable and necessary constraint to the scaling of TWS signals over a particular study area as no consistent basis for ground-truthing these factors exists.

The disaggregation of GRACE-derived ΔTWS anomalies into individual water stores (Eq. 1) is commonly constrained by the limited availability of observations of terrestrial freshwater stores (i.e., ΔSWS, ΔSMS, ΔGWS, ΔISS). Indeed, a major source of uncertainty in the attribution of GRACE ΔTWS derives from the continued reliance on modelled ΔSMS derived from LSMs (i.e., CLM, NOAH, VIC, MOSAIC) under the Global Land Data Assimilation System or GLDAS (Rodell et al., 2004) and remote-sensing products (Shamsudduha et al., 2012; Khandu et al., 2016). Further, analyses of GRACE-derived ΔGWS often assume ΔSWS is limited (Kim et al., 2009) yet studies in the humid tropics and engineered systems challenge this assumption showing that it can overestimate ΔGWS (Shamsudduha et al., 2012; Longuevergne et al., 2013). Robust estimates of ΔGWS from GRACE gravity signals have, to date, been developed in locations where ΔSWS is well constrained by in situ observations and groundwater is used intensively for irrigation so that ΔGWS comprises a significant (>10 %) proportion of ΔTWS (Leblanc et al., 2009; Famiglietti et al., 2011; Shamsudduha et al., 2012; Scanlon et al., 2015). In Sub-Saharan

105 Africa, intensive groundwater withdrawals are restricted to a limited number of locations
106 (e.g., irrigation schemes, cities) and constrained by low-storage, low-transmissivity aquifers
107 in the deeply weathered crystalline rocks that underlie ~40 % of this region (MacDonald et
108 al., 2012) including the Upper Nile Basin (Fig. 1). Consequently, the ability of low-resolution
109 GRACE gravity signals to trace ΔGWS in these hard-rock environments is unclear. A recent
110 study (Nanteza et al., 2016) applies NASA's *GRCTellus* (CSR GRACE) data over large basin
111 areas (>300 000 km^2) of East Africa and argues that ΔGWS can be estimated with sufficient
112 reliability to characterise regional groundwater systems after accounting for ΔSWS by
113 satellite altimetry and ΔSMS data from the GLDAS LSM ensemble (Rodell et al., 2004).
114
115 Here, we exploit a large-scale reduction and recovery in surface water storage that was
116 recorded within Lake Victoria (Fig. 1), the world's second largest lake by surface area (67
117 220 km^2) (UNEP, 2013) and eighth largest by volume (2 760 km^3) (Awange et al., 2008).
118 This well-constrained reduction in ΔSWS comprises a decline in lake level of 1.2 m between
119 May 2004 and February 2006, equivalent to a lake-water volume (ΔSWS) loss of 81 km^3 that
120 resulted, in part, from excessive dam releases (Fig. 2). We test the ability of current GRACE
121 products to represent the amplitude and phase of this voluminous and well-constrained
122 change in freshwater storage. Our analysis focuses on both the Lake Victoria Basin (hereafter
123 LVB) (256 100 km^2) and Lake Kyoga Basin (hereafter LKB) (79 270 km^2) (Fig. 1). Applying
124 in situ observations of ΔSWS and ΔGWS combined with simulated ΔSMS by the GLDAS
125 LSMs, we assess: (1) the ability of current gridded GRACE products (i.e., *GRCTellus*, JPL-
126 Mascons, GRGS GRACE) to measure a well constrained ΔTWS in the Upper Nile Basin
127 from 2003 to 2012 focusing on the unintended experiment within the LVB from 2003 to
128 2006; and (2) the sensitivity of a disaggregated GRACE ΔTWS signals to trace ΔGWS in a
129 deeply weathered crystalline rock aquifer systems underlying the Upper Nile Basin.

2. The Upper Nile Basin

2.1 Hydroclimatology

The Upper Nile Basin, the headwater area of the ~3 400 000 km^2 Nile Basin (Awange et al., 2014), includes both the Lake Victoria Basin (LVB) and Lake Kyoga Basin (LKB). Mean annual rainfall over the entire basin varies from 650 to 2900 mm (TRMM monthly rainfall; 2003–2012) with an average of 1300 mm and standard deviation of 354 mm (Fig. 3). Mean annual gauged rainfall at different stations, Jinja, Bugondo and Entebbe measured is 1195, 1004 and 1541 mm, respectively (Owor et al., 2011). Rainfall over Lake Victoria is typically 25–30 % greater than that measured in the surrounding catchment (Fig. 3), which is partially explained by the nocturnal 'lake breeze' effect (Yin and Nicholson, 1998; Nicholson et al., 2000; Owor et al., 2011).

Estimates of mean annual evaporation from the surface of Lake Victoria vary from 1260 mm (UNEP, 2013) to 1566 mm (Hoogeveen et al., 2015) whereas mean annual evaporation from the surface of Lake Kyoga is estimated to vary from 1205 mm (Brown and Sutcliffe, 2013) to 1660 mm (Hoogeveen et al., 2015). Evapotranspirative fluxes from the surrounding swamps in Lake Kyoga are estimated to be much higher and approximately 2230 mm yr^{-1} (Brown and Sutcliffe, 2013).

Annual rainfall is predominantly bimodal in distribution (Fig. 4) with two distinct rainy seasons driven by the movement of the Intertropical Convergence Zone (ITCZ) (Awange et al., 2013). Long rains (March to May) and short rains (September to November) account for approximately 40% and 25% of annual rainfall respectively (Basalirwa, 1995; Indeje et al., 2000). The latter rainfalls are particularly influenced by El-Niño Southern Oscillation

(ENSO) and Indian Ocean Dipole (IOD). GRACE-derived ΔTWS within the LVB shows a statistical association (R^2) of 0.56 with ENSO and 0.48 with IOD (Awange et al., 2014).

2.2 Lakes Victoria and Kyoga

Located between 31°39' E and 34°53' E longitudes, and 0°20' N and 3°00' S latitudes, Lake Victoria (Fig. 1) is located in Tanzania, Uganda and Kenya where each accounts for 51 %, 43 % and 6 % of lake surface area respectively (Kizza et al., 2012). Lake Victoria is relatively shallow with a mean depth of ~40 m and a maximum depth of 84 m (UNEP, 2013) akin to many shallow, open surface-water bodies as well as permanent and seasonal wetlands occupying low relief plateau across the Great Lakes Region of Africa (Owor et al., 2011). Moreover, the western and northwestern lake bathymetry is characterised by even shallower depths of between 4 and 7 m (Owor, 2010). Hydrologically, lake input is dominated by direct rainfall (84 % of total input); the remainder derives primarily from river inflows as direct groundwater inflow (<1 %) is negligible (Owor et al., 2011). Approximately 25 major rivers flow into Lake Victoria with a total catchment area of ~194 000 km^2; the largest tributary, River Kagera, contributes ~30 % of total river inflows (Sene and Plinston, 1994). Lake Victoria outflow to Lake Kyoga occurs at Jinja (Fig. 1).

Lake Kyoga (Fig. 1), located between 32°10' E and 34°20' E longitudes, and 1°00' N and 2°00' N latitudes, has a mean area of 1 720 km^2 with an estimated mean volume of 12 km^3 (Owor, 2010; UNEP, 2013). According to the recent global *HydroSHEDS* (Hydrological data and maps based on shuttle elevation derivatives at multiple scales) database, the Lake Kyoga has a total surface area of 2 729 km^2 (Lehner et al., 2008). Lake Kyoga comprises lake-zone and flow-through conduit areas. The lake zone in Lake Kyoga is very shallow with a mean depth of 3.5 to 4.5 m (Owor, 2010). Lake Kyoga has a through-flow channel (mean depth 7

to 9 m) where the main Victoria Nile River flows (Owor, 2010) and acts as a linear reservoir with the annual water balance predominantly governed by the discharge of the Victoria Nile from Lake Victoria. Lake Kyoga has a through-flow channel (mean depth 7–9 m) where the main Victoria Nile River flows (Owor, 2010). Whilst numerous rivers flow into Lake Kyoga (e.g. Rivers Mpologoma, Awoja, Omunyal, Abalang, Olweny, Sezibwa and Enget) (Owor, 2010), the majority contributes a fraction of their former volume upon reaching the lake (Krishnamurthy and Ibrahim, 2013) due, in part, to evapotranspirative losses from fringe swamp areas (4 510 km^2) surrounding the lake (UNEP, 2013).

2.3 Hydrogeological setting

The Upper Nile Basin is underlain primarily by deeply weathered crystalline rock aquifer systems that have evolved through long-term, tectonically-driven cycles of deep weathering and erosion (Taylor and Howard, 2000). Groundwater occurs within unconsolidated regoliths or 'saprolite' and, below this, in fractured bedrock, known as 'saprock'. Bulk transmissivities of the saprolite and saprock aquifers are generally low (1 to 20 m^2 d^{-1}) (Taylor and Howard, 2000; Owor, 2010) and field estimates of the specific yield of the saprolite, the primary source of groundwater storage in these aquifer systems, are 2 % based on pumping-tests with tracers (Taylor et al., 2010) and magnetic resonance sounding experiments (Vouillamoz et al., 2014). Borehole yields are highly variable but generally low (0.5 to 20 m^3 h^{-1}) yet are of critical importance to the provision of safe drinking water.

2.4 An observed reduction in TWS in the LVB

In 1954, the construction of the Nalubaale Dam (formerly Owen Falls Dam) at the outlet of Lake Victoria at Jinja transformed the lake into a controlled reservoir (Sene and Plinston, 1994). Operated as a run-of-river hydroelectric project to mimic pre-dam outflows, the

205 'Agreed Curve' between Uganda and Egypt dictated dam releases that were controlled on a
206 10-day basis and generally adhered to, with compensatory discharge releases to minimise any
207 departures, until the construction of the Kiira dam at Jinja in 2002 (Sene and Plinston, 1994;
208 Owor et al., 2011).
209
210 The combined discharge of the Nalubaale and Kiira Dams enabled total dam releases (Fig. 2)
211 to substantially exceed the Agreed Curve (Sutcliffe and Petersen, 2007) and between May
212 2004 and February 2006 the lake level dropped by 1.2 m (equivalent ΔSWS loss of 81 km^3)
213 (Owor et al., 2011). Mean annual releases were 1387 $m^3 s^{-1}$ (+162 % of Agreed Curve) in
214 2004 and 1114 $m^3 s^{-1}$ (+148 % of Agreed Curve) in 2005. Sharp reductions in dam releases in
215 2006 helped to arrest and reverse the lake-level decline with lake levels stabilising by early
216 2007.
217
218 **3. Data and Methods**
219 **3.1 Datasets**
220 We use publicly available time-series records of: (1) GRACE TWS solutions from a number
221 of data-processing strategies and dissemination centres including NASA's *GRCTellus* land
222 solutions [RL05 for CSR, GFZ (version DSTvSCS1409), RL05.1 for JPL (version
223 DSTvSCS1411) and JPL-Mascons solution (version RL05M_1.MSCNv01)]as well as the
224 French National Centre for Space Studies (CNES) GRGS solution (version GRGS RL03-v1);
225 (2) NASA's Global Land Data Assimilation System (GLDAS) simulated soil moisture data
226 from 3 global land surface models (LSMs) (CLM, NOAH, VIC); and (3) monthly
227 precipitation data from NASA's Tropical Rainfall Measuring Mission (TRMM) satellite
228 mission. We also employ in-situ observations of lake levels and groundwater levels from a

network of river gauges and monitoring boreholes operated by the Ministry of Water and Environment in Entebbe (Uganda). Datasets are briefly described below.

3.1.1 Delineation of basin study areas

Delineation of the Lake Victoria Basin (LVB) and Lake Kyoga Basin (LKB) was conducted in Geographic Information System (GIS) environment under ArcGIS (v.10.3.1) environment using the 'Hydrological Basins in Africa' datasets derived from *HydroSHEDS* database (available at http://www.hydrosheds.org/) (Lehner et al., 2006, 2008). Regional water bodies including Lakes Victoria and Kyoga (Fig. 1) were spatially defined by the Inland Water dataset available globally at country scale from DIVA-GIS (Hijmans et al., 2012). Computed areas of the basins and lake surface areas are summarised in Table 1 along with previously estimated figures from other studies.

3.1.2 GRACE-derived terrestrial water storage (TWS)

Twin GRACE satellites provide monthly gravity variations interpretable as ΔTWS (Tapley et al., 2004) with an accuracy of ~1.5 cm (Equivalent Water Thickness or Depth) when spatially averaged (Wahr et al., 2006). In this study, we apply 5 different monthly GRACE solutions for the period of January 2003 to December 2012: post-processed, gridded (1° × 1°) GRACE-TWS time-series records from 3 *GRCTellus* land solutions from CSR, JPL and GFZ processing centres (available at http://grace.jpl.nasa.gov/data) (Swenson and Wahr, 2006; Landerer and Swenson, 2012), JPL-Mascons (Watkins et al., 2015; Wiese et al., 2015), and GRGS GRACE products (CNES/GRGS release RL03-v1) (Biancale et al., 2006).

GRCTellus land solutions are post-processed from two versions, RL05 and RL05.1 of spherical harmonics released by the University of Texas at Austin Centre for Space Research

(CSR) and the German Research Centre for Geosciences Potsdam (GFZ), and the NASA's Jet Propulsion Laboratory (JPL) respectively. *GRCTellus* gridded datasets are available at monthly timestep at a spatial resolution of 1° × 1° (~111 km at equator) though the actual spatial resolution of GRACE footprint is ~450 km or ~200,000 km^2 (Scanlon et al., 2012). Post-processing of *GRCTellus* GRACE datasets primarily involve (i) removal of atmospheric pressure or mass changes based on the European Centre for Medium-Range Weather Forecasts (ECMWF) model; (ii) a glacial isostatic adjustment (GIA) correction based on a viscoelastic 3-D model of the Earth (A et al., 2013); and (iii) an application a destriping filter plus a 300-km Gaussian to minimise the effect of correlated errors (i.e., destriping) manifested by N-S elongated stripes in GRACE monthly maps. However, the use of a large spatial filter and truncation of spherical harmonics leads to energy removal so scaling coefficients or factors are applied to the *GRCTellus* GRACE -derived TWS data in order to restore attenuated signals (Landerer and Swenson, 2012). Dimensionless scaling factors are provided as 1° × 1° bins (see supplementary Fig. S1) that derive from the Community Land Model (CLM4.0) (Landerer and Swenson, 2012).

JPL-Mascons (version RL05M_1.MSCNv01) data processing also involves a glacial isostatic adjustment (GIA) correction based on a viscoelastic 3-D model of the Earth (A et al., 2013). JPL-Mascons applies no spatial filtering as JPL-RL05M directly relates inters-satellite range-rate data to mass concentration blocks or Mascons to estimate global monthly gravity fields in terms of equal area 3° × 3° mass concentration functions to minimise measurement errors. The use of Mascons and the special processing result in better signal-to-noise ratios of the mascon fields compared to the conventional spherical harmonic solutions (Watkins et al., 2015). For convenience, gridded Mascons fields are provided at a spatial sampling of 0.5° in both latitude and longitude (~56 km at the equator). As with *GRCTellus* GRACE datasets the

neighbouring grid cells are not 'independent' of each other and cannot be interpreted individually at the 1° or 0.5° grid scale (Watkins et al., 2015). Similar to *GRCTellus* GRACE (CSR, JPL, GFZ) products, dimensionless scaling factors are provided as 0.5° × 0.5° bins (see supplementary Fig. S2) that also derive from the Community Land Model (CLM4.0) (Wiese et al., 2016). The gain factors or scaling coefficients are multiplicative factors that minimize the difference between the smoothed and unfiltered monthly ΔTWS variations from 'actual' land hydrology at a given geographical location (Wiese et al., 2016).

GRGS/CNES GRACE monthly products (version RL03-v1) are processed and made publicly available (http://grgs.obs-mip.fr/grace) by the French Government space agency, National Centre for Space Studies or Centre National d' Études Spatiales (CNES). The post-processing of GRGS data involves taking into account of gravitational variations such as Earth tides, ocean tides, and 3D gravitational potential of the atmosphere and ocean masses (Bruinsma et al., 2010). The remaining signals for time-varying gravity fields therefore represent changes in terrestrial hydrology including snow cover, baroclinic oceanic signals and effects of post-glacial rebound (Biancale et al., 2006; Lemoine et al., 2007). Further details on the Earth's mean gravity-field models can be found on the official website of GRGS/LAGEOS (http://grgs.obs-mip.fr/grace/).

GRACE satellites were launched in 2002 to map the variations in Earth's gravity field over its 5-year lifetime but both satellites are still in operation even after more than 14 years. However, active battery management since 2011 has led the GRACE satellites to be switched off every 5−6 months for 4−5 week durations in order to extend its total lifespan (Tapley et al., 2015). As a result, GRACE ΔTWS time-series data have some missing records that are linearly interpolated (Shamsudduha *et al*., 2012). In this study, we derive ΔTWS time-series

304 data as equivalent water depth (cm of H_2O) using the basin boundaries (GIS shapefiles) for
305 masking the 1° × 1° grids.
306
307 **3.1.3 Rainfall data**
308 We apply Tropical Rainfall Measuring Mission (TRMM) (Huffman et al., 2007) monthly
309 product (3B43 version 7) for the period of January 2003 to December 2012 at 0.25° × 0.25°
310 spatial resolution and aggregate to 1° × 1° grids over LVB and LKB. General climatology of
311 the Upper Nile Basin is represented by long-term (2003–2012) mean annual rainfall (Fig. 3)
312 and seasonal rainfall pattern (Fig. 4). TRMM rainfall measurements show a good agreement
313 with limited observational precipitation records (Awange et al., 2008; Awange et al., 2014).
314
315 **3.1.4 Soil moisture storage (SMS)**
316 NASA's Global Land Data Assimilation System (GLDAS) is an uncoupled land surface
317 modelling system that drives multiple land surface models (GLDAS LSMs: CLM, NOAH,
318 VIC and MOSAIC) globally at high spatial and temporal resolutions (3-hourly to monthly at
319 0.25° × 0.25° grid resolution) and produces model results in near-real time (Rodell et al.,
320 2004). These LSMs provide a number of output variables which include soil moisture storage
321 (SMS). Similar to the approach applied in the analysis of GRACE-derived ΔTWS analysis in
322 the Bengal Basin (Shamsudduha et al., 2012), we apply simulated monthly ΔSMS records at
323 a spatial resolution of 1° × 1° from 3 GLDAS LSMs: the Community Land Model (CLM,
324 version 2) (Dai et al., 2003), NOAH (version 2.7.1) (Ek et al., 2003) and the Variable
325 Infiltration Capacity (VIC) model (version 2.7.1) (Liang et al., 2003). The respective depths
326 of modelled soil profiles are 3.4 m, 2.0 m, and 1.9 m in CLM (10 vertical layers), NOAH (4
327 vertical layers), and VIC (version 1.0) (3 vertical layers). Because of the absence of in situ
328 soil moisture data in the study areas we apply an ensemble mean of the aforementioned 3

329 LSMs-derived simulated ΔSMS time-series records (see Figs. 5 and 6) in order to
330 disaggregate GRACE ΔTWS signals in LVB and LKB.
331
332 **3.1.5 Surface water storage (SWS)**
333 Daily time-series of ΔSWS are computed from in situ (gauged) lake-level observations at
334 Jinja for Lake Victoria and Bugondo for Lake Kyoga (Figs. 1 and 2) compiled by the
335 Ugandan Ministry of Water and Environment (Directorate of Water Resources Management).
336 Mean monthly anomalies for the period of January 2003 – December 2012 were computed as
337 an equivalent water depth using Eq. (2). Missing data in the time series (2003–2012) records
338 are linearly interpolated. For instance, in case of monthly ΔSWS derived from Lake Kyoga
339 water levels, there is one missing record (December 2005).
340
341 $$\Delta SWS = \Delta Lake\ Level \times \left(\frac{Lake\ Area}{Total\ Basin\ Area}\right) \quad (2)$$
342
343 **3.1.6 Groundwater storage (GWS) from borehole observations**
344 Time series of ΔGWS are constructed from in situ piezometric records from 6 monitoring
345 wells located in LVB and LKB where near-continuous, daily observations exist from January
346 2003 to December 2012 and have been compiled by the Ugandan Ministry of Water and
347 Environment (Directorate of Water Resources Management) (Owor et al., 2009; Owor et al.,
348 2011). Monitoring boreholes were installed into weathered, crystalline rock aquifers that
349 underlie much of LVB and LKB, and are remote from local abstraction. As such, they
350 represent variations in groundwater storage influenced primarily by climate variability. Mean
351 monthly anomalies of ΔGWS, standardised to mean records from January 2003 to December
352 2012, were derived from near-continuous, daily observations at Entebbe, Rakai and
353 Nkokonjeru for LVB and at Apac, Pallisa and Soroti for LKB (Fig. 1; Table 2; see

354 supplementary Fig. S3). In the Lake Kyoga Basin, piezometric records from 3 sites show
355 consistency in the seasonality and amplitude of groundwater storage changes plotted as
356 monthly groundwater-level anomalies relative to the mean for the period from January 2003
357 to December 2012. In the Lake Victoria Basin, groundwater-level records from 2 sites
358 (Entebbe, Nkokonjeru) are similar in their phase and amplitude, and are influenced by
359 changes in the level of Lake Victoria as demonstrated by Owor et al. (2011). The
360 groundwater-level record from Rakai represents local semi-arid conditions that exist within
361 catchment areas (e.g., River Ruizi) draining to the western shore of Lake Victoria in Uganda.
362 Although there are differences in the phase of groundwater-level fluctuations between the
363 semi-arid site at Rakai and both Entebbe and Nkokonjeru (as well as the 3 sites in the Lake
364 Kyoga Basin), annual amplitudes are similar.
365
366 The groundwater-level time series data are a sub-set of the total number of available
367 monitoring-well records in the LVB and LKB and selected on the basis of (i) the
368 completeness and quality of the records from 2003 to 2012, and (ii) rigorous review of
369 groundwater-level records conducted at a dedicated workshop at the Ministry of Water &
370 Environment in January 2013. These records represent shallow groundwater-level
371 observations within the saprolite that is dynamically connected to surface waters (Owor et al.
372 2011). Long time-series records of groundwater levels over the period from 2003 to 2012
373 from western Kenya, northern Tanzania, Rwanda and Burundi have not been identified
374 despite intensive investigations carried out by *The Chronicles Consortium*[1]. The partial
375 spatial coverage in quality-controlled piezometry, especially for the LVB, represents an
376 important limitation in our analysis.
377

[1] The Chronicles Consortium: https://www.un-igrac.org/special-project/chronicles-consortium

Mean monthly anomalies were translated into an equivalent water depth (Eq. 3) by applying a range of specific yield (S_y) values (1–6 % with an average of 3 %) although estimates of S_y in hard-rock environments are observed to vary from < 2% to 8 % (Taylor et al., 2010; Taylor et al., 2013; Vouillamoz et al., 2014) using Eq. (3). Missing data in the time series were linearly interpolated. In case of monthly ΔGWS that derived from borehole (n=6) observations, missing records range from 1–9 months (120 months in 2003–2012) with three boreholes (Soroti, Rakai and Nkonkonjero) with time-series records ending in June–July 2010.

$$\Delta GWS = \Delta h * S_y * \left(\frac{Land\ Area}{Total\ Basin\ Area}\right) \quad (3)$$

3.2 Methodologies

3.2.1 GRACE ΔTWS estimation

First, the 1° × 1° gridded monthly anomalies of GRACE-derived ΔTWS and GLDAS LSMs derived ΔSMS are masked over the area of LVB and LKB. GRACE ΔTWS along with GLDAS ΔSMS are extracted for the marked 1° × 1° grid cells for LVB and LKB and the grid values are spatially aggregated to form time-series of monthly anomalies ΔTWS and ΔSMS.

GRCTellus GRACE ΔTWS gridded data are scaled using dimensionless, gridded scaling factors. Several GRACE studies (Rodell et al., 2009; Sun et al., 2010; Shamsudduha et al., 2012) have applied scaling factors in three different ways: (1) single scaling factor based on regionally averaged time series, (2) spatially distributed or gridded scaling factors based on time-series at each grid point, and (3) gridded-gain factors estimated as a function time or of temporal frequency (Landerer and Swenson, 2012; Long et al., 2015).. In this study, we apply spatially-distributed scaling approach (method 2 above) to generate basin-averaged ΔTWS time-series records for *GRCTellus* (CSR, JPL, GFZ) products. Scaling factors provided at 1°

403 × 1° grids are applied to each corresponding GRACE ΔTWS grids for NASA's *GRCTellus*
404 products in order to restore attenuated signals during the post-processing (Landerer and
405 Swenson, 2012) using Eq. (4). Similarly, provided scaling factors are applied to JPL-
406 Mascons ΔTWS time-series data but at 0.5° × 0.5° grid resolution. No scaling factors were
407 applied to GRGS GRACE ΔTWS as the monthly gravity solutions have already been
408 stabilised during their generation process.
409
410 $$g^1(x, y, t) = g(x, y, t) \times s(x, y) \quad (4)$$
411
412 Here, $g^1(x, y, t)$ represents each un-scaled grid where x represents longitude, y represents
413 latitude, and t represents time (month), and $s(x, y)$ is the corresponding scaling factor.
414
415 For the 3 *GRCTellus* gridded products (i.e., CSR, GFZ, and JPL solutions), we apply an
416 ensemble mean of scaled GRACE ΔTWS as our exploratory analyses reveal that ΔTWS
417 time-series records over the Lake Victoria Basin are highly correlated (r >0.95, p-value
418 <0.001) to each other. Additionally, small (ranges from 1.3 to 1.9 cm) Root Mean Square
419 Error (RMSE) among the GRACE ΔTWS datasets suggests substantial similarities in phase
420 and amplitude.
421
422 **3.2.2 Estimation of ΔGWS from GRACE**
423 Estimation of groundwater storage changes (ΔGWS) from GRACE measurements is
424 conducted using Eq. (5) in which ΔTWS_t is derived from gridded GRACE products (spatially
425 scaled ΔTWS for *GRCTellus* and JPL-Mascons but unscaled ΔTWS for GRGS), ΔSMS_t is an
426 ensemble mean of 3 GLDAS LSMs (CLM, NOAH, VIC), and ΔSWS_t is area-weighted, in-
427 situ surface water storage estimated from lake-level records using Eq. (2).

$$\Delta \mathrm{G}WS_t = \Delta TWS_t - (\Delta SWS_t + \Delta SMS_t) \quad (5)$$

3.2.3 Reconciliation of GRACE ΔTWS disaggregation

Reconciling GRACE-derived TWS with ground-based observations is limited by the paucity of in situ observations of SMS, SWS and GWS in many environments. In addition, direct comparisons between in situ observations of ΔSMS, ΔSWS and ΔGWS and gridded GRACE ΔTWS anomalies are complicated by substantial differences in spatial scales, which need to be considered prior to analysis (Becker et al., 2010). For example, individual groundwater-level monitoring boreholes may represent, depending on borehole depth, a sensing area of several 10s of km^2 (Burgess et al., 2017), whereas the typical GRACE footprint is ~200 000 km^2. The disaggregation of GRACE ΔTWS into individual water store can also propagate errors to disaggregated components. Here, we construct 'in situ' or 'bottom-up' ΔTWS (i.e., combined signals of ΔSMS, ΔSWS and ΔGWS) for the Lake Victoria Basin and attempt to reconcile with GRACE-derived ΔTWS. One feature of GRACE ΔTWS among the 3 solutions we apply in this study is the considerable variation in annual amplitudes that exist over the period of 2003 to 2012.

In addition, for the *GRCTellus* products, we conduct unconventional scaling experiments, outlined below in an attempt to reconcile satellite and in situ measures and to shed light on the uncertainty in ΔTWS amplitudes of the *GRCTellus* GRACE products. The ΔTWS signals in CSR, JPL and GFZ products is greatly attenuated due to spatial smoothing and the amplitude is substantially smaller compared to JPL-Mascons and GRGS products. In the first scaling experiment, we apply an additional, basin-averaged, multiplicative scaling factor to ΔTWS ranging from 1.1 to 2.0 and employ RMSE to assess their relative performance. With

reference to *GRCTellus* GRACE ΔTWS and bottom-up ΔTWS relationship, the scaling factor producing the lowest RMSE between the two time series is employed. Secondly, it is observed that in the LVB, ΔSWS is the largest contributor, representing ~50% variance in the in-situ or bottom-up ΔTWS time-series signal. GRACE ΔTWS analyses commonly apply the same scaling factor as ΔTWS to all other individual components (Landerer and Swenson, 2012). Therefore, under the scaling experiment, we apply to in-situ ΔSWS spatially-averaged scaling factors representative of (i) Lake Victoria and its surrounding grid cells (experiment 1: s=0.71; range 0.02−1.5), and (ii) the open-water surface of Lake Victoria without surrounding grid cells (experiment 2: s=0.11; range 0.02−0.30). Furthermore, we find that the amplitude of monthly anomalies of ΔSWS+ΔSMS combined substantially exceed ΔTWS (see supplementary Fig. S4), particularly for the *GRCTellus* GRACE ΔTWS signal that is greatly smoothed due to filtering. This discrepancy is pronounced over the period of 2003−2006, and when applied to estimate GRACE-derived ΔGWS, produces steep, rising trends in the estimated ΔGWS (i.e., GRACE ΔTWS − (ΔSWS+ΔSMS)) whereas borehole observations of groundwater levels show declining trend and of much lower amplitude over the same period.

4. Results

Monthly time-series records (January 2003 to December 2012) are presented in Figures 5 and 6 respectively for Lake Victoria Basin (LVB) and Lake Kyoga Basin (LKB) of (a) GRACE ΔTWS from *GRCTellus* GRACE ΔTWS (ensemble mean of CSR, GFZ, and JPL solutions), GRGS and JPL-Mascons, (b) GLDAS land surface models (LSMs) derived ΔSMS (ensemble mean of 3 LSMs: NOAH, CLM, VIC), (c) in situ ΔSWS from lake levels records, and (d) in situ ΔGWS borehole observations. Monthly rainfall derived from TRMM satellite observations over the same period are shown on the bottom panel (d). Time-series records of all ΔTWS components and rainfall are aggregated for LVB to represent the average seasonal

478 (monthly) pattern of each signal (Fig. 4) that shows an obvious lag (~1 month) between peak
479 rainfall (March−April) and ΔTWS and its individual components.

480

481 Mean annual (2003−2012) amplitudes of various GRACE-derived ΔTWS signals, bottom-up
482 ΔTWS, ensemble mean of simulated ΔSMS, in situ ΔSWS and ΔGWS time-series records
483 (Figs. 5 and 6) are presented (see supplementary Table S1) for both LVB and LKB. Mean
484 annual amplitude of GRACE ΔTWS ranges from 11 to 21 cm among *GRCTellus*, GRGS and
485 JPL-Mascons GRACE products in LVB, and from 8.4 to 16.4 respectively in LKB. Mean
486 annual amplitude of in situ ΔSWS is much greater (14.8 cm) in LVB than in LKB (3.8 cm).
487 GLDAS LSMs derived ensemble mean ΔSMS amplitude in LVB is 7.9 cm and 7.3 cm in
488 LKB. The standard deviation in ΔSMS varies substantially in LVB (1.2 cm, 4.2 cm, and 2.9
489 cm) LKB (1.3 cm, 4.7 cm, and 4.0 cm) for CLM, NOAH, and VIC models respectively.
490 Mean annual amplitude of in situ ΔGWS ranges from 4.4 cm (LVB) to 3.5 cm (LKB).

491

492 Time-series correlation (Pearson) analysis over various periods of interests (decadal: 2003–
493 2012; well-constrained SWS reduction or a period of unintended experiment: 2003–2006;
494 controlled dam operation: 2007–2012) reveals that GRACE-derived ΔTWS signals are
495 strongly correlated in both LVB and LKB (see supplementary Figs. S5–S10). For example, in
496 LVB, in situ ΔSWS shows a statistically significant (p-value <0.001) strong correlation
497 (r=0.77–0.92) with all GRACE- ΔTWS time-series (2003–2012) records. Similarly,
498 simulated ΔSMS shows statistically significant (p-value <0.001) strong correlation (r=0.70–
499 0.78) with ΔTWS time-series records. In contrast, in situ ΔGWS shows statistically
500 significant (p-value <0.001) but moderate correlation (r=0.63–0.69) with ΔTWS time-series
501 records. Correlation among the variables shows similar statistically significant (p-value

<0.001) but wide-ranging associations for the periods of unintended experiment (2003–2006) and controlled dam operation (2007–2012). In LKB, however, correlation among in situ ΔSWS and GRACE ΔTWS time-series records is statistically significant (p-value <0.05) but poor in correlation strength (r=0.22–0.34). In situ ΔGWS shows statistically significant (p-value <0.001) strong correlation (r=0.64–0.69) with GRACE ΔTWS time-series records.

Time-series records of all 3 ΔTWS from 5 GRACE products and bottom-up ΔTWS time-series records in both LVB and LKB are shown in Figure 7 and results of temporal trends are summarised in Table 3. Statistically significant (p-value <0.05) declining trends (–4.1 to –11.0 cm yr^{-1} in LVB; –2.1 to –4.6 cm yr^{-1} in LKB) are consistently observed during the period of 2003 to 2006. Trends are all positive in GRACE ΔTWS and bottom-up ΔTWS time-series records over the recent period of controlled dam operation (2007–2012) in both LVB and LKB. Therefore, the overall, decadal (2003–2012) trends are slightly rising (0.04 to 1.00 cm yr^{-1}) in LVB but nearly stable (–0.01 cm yr^{-1}) in *GRCTellus* ΔTWS and slightly declining (–0.56 cm yr^{-1}) bottom-up ΔTWS over LKB. In addition, short-term volumetric trends (2003–2006) in GRACE and bottom-up ΔTWS as well as simulated ΔSMS and in situ ΔSWS are declining whereas in situ ΔGWS and rainfall anomalies show slightly rising trends over the same period in LVB (see supplementary Figs. S11–S12). Similar trends are reported in various signals over LKB but magnitudes are much smaller compared to that of LVB, which is 3 times larger in size than LKB. Volumetric declines in ΔTWS in the LVB for the period 2003 to 2006 are: 83 km^3 (bottom-up), 80 km^3 (JPL-Mascons), 69 km^3 (GRGS) and 31 km^3 (*GRCTellus* ensemble mean of CSR, JPL and GFZ products).

525 Linear regression reveals that the association between GRACE-derived ΔTWS and bottom-up
526 ΔTWS is stronger in LVB (R^2=0.75–0.90) than in LKB (R^2=0.56–0.62) (see supplementary
527 Table S1). GRACE ΔTWS is unable to explain natural variability in bottom-up ΔTWS in
528 LKB though this may be explained by the fact that SWS in Lake Kyoga is influenced by dam
529 releases from LVB. Multiple linear regression and the Analysis of Variance (ANOVA) reveal
530 that the relative proportion of variability in bottom-up ΔTWS time-series record can be
531 explained by ΔSWS (92.6 %), ΔSMS (6.5 %) and ΔGWS (0.66 %) in LVB; and by 47.9 %,
532 48.5 % and 3.6 % respectively in LKB. These results are indicative only as these percentages
533 can be biased by the presence of strong correlation among variables and the order of these
534 variables listed as predictors in the multiple linear regression models.

535

536 Disaggregation of ΔGWS from GRACE ΔTWS time-series record from each product has
537 been carefully considered and estimated following Eq. (5). No further additional scaling
538 factors, as described in the 'scaling experiment' section (see results of scaling experiment in
539 supplementary Fig. 13) are applied in the final disaggregation of ΔGWS from GRACE
540 ΔTWS signals. Results of Pearson correlation analysis of the time-series record (2003–2012)
541 of in situ ΔGWS in LVB show statistically insignificant and poor correlation (r=0.11, p-value
542 0.25) to JPL-Mascons and an inverse correlation with both the ensemble *GRCTellus*
543 (r=–0.55, p-value <0.001) and GRGS (r=–0.27, p-value=0.003) GRACE-derived estimates
544 of ΔGWS (Fig. 8). In contrast, in LKB, in situ ΔGWS time-series record shows statistically
545 significant but weak correlations to JPL-Mascons (r=0.34, p-value <0.001) and GRGS
546 (r=0.39, p-value <0.001) GRACE-derived ΔGWS but shows an inverse correlation (r=–0.21,
547 p-value=0.02) to *GRCTellus* ΔGWS (see supplementary Fig. S14). Furthermore, RMSE
548 among various GRACE-derived estimates of ΔGWS and in situ ΔGWS ranges from 7.2 cm

549 (GRACE ensemble), 3.8 cm (GRGS) to 8.2 cm (JPL-Mascons) in LVB, and from 3.2
550 (GRACE ensemble), 5.3 cm (GRGS) to 5.4 cm (JPL-Mascons) in LKB.

551

552 **5. Discussion**

553 We apply 5 different gridded GRACE products (*GRCTellus* – CSR, JPL and GFZ; GRGS
554 and JPL-Mascons) to test ΔTWS signals for in the Lake Victoria Basin (LVB) comprising a
555 large and accurately observed reduction (83 km^3) in ΔTWS from 2003 to 2006. Our analysis
556 reveals that all GRACE products capture this substantial reduction in terrestrial water mass
557 but the magnitude of GRACE ΔTWS among GRACE products varies substantially. For
558 example, *GRCTellus* underrepresents greatly (63 %) the reduction of 83 km^3 in bottom-up
559 ΔTWS whereas GRGS and JPL-Mascons GRACE products underrepresent this by 17 % and
560 4 % respectively. Over a longer period (2003−2012) in the Upper Nile Basin, all GRACE
561 products correlate well with bottom-up ΔTWS but, similar to the unintended experiment,
562 variability in amplitude is considerable (Fig. 9). The average (2003−2012) annual amplitude
563 of ΔTWS is substantially dampened (i.e., 45 % less than bottom-up ΔTWS) in *GRCTellus*
564 GRACE products relative to GRGS (4 %) and JPL-Mascons (27 % more than bottom-up
565 ΔTWS) products in the LVB.

566

567 The 'true' amplitude in *GRCTellus* ΔTWS signal is generally reduced during the post-
568 processing of GRACE spherical harmonic fields, primarily due to spatial smoothing by a
569 large-scale (e.g., 300 km) Gaussian filter and truncation of gravity fields at a higher (degree
570 60 = 300 km) spectral degree (Swenson and Wahr, 2006; Landerer and Swenson, 2012).
571 Despite the application of scaling factors based on CLM v.4.0 to amplify *GRCTellus* ΔTWS
572 amplitudes at individual grids, the basin-averaged (LVB) time-series record represents only

573 75 % variability in bottom-up ΔTWS. Scaling experiments conducted here reveal that
574 *GRCTellus* ΔTWS requires an additional multiplicative factor of 1.7 in order to match
575 bottom-up ΔTWS with a minimum RMSE (5.8 cm). On the other hand, NASA's new gridded
576 GRACE product, JPL-Mascons, that applies a priori constraint in space and time to derive
577 monthly gravity fields and undergoes some degree of spatial smoothing (Watkins et al.,
578 2015), represents nearly 83 % variability in bottom-up ΔTWS. In contrast, the GRGS
579 GRACE product, which applies truncation at degree 80 (~250 km) does not suffer from any
580 large-scale spatial smoothing, and is able to represent well (90 %) the variability in bottom-
581 up ΔTWS in the LVB.

582

583 A priori corrections of *GRCTellus* ensemble mean GRACE signals using a set of LSM-
584 derived scaling factors (i.e., amplitude gain) can lead to substantial uncertainty in ΔTWS
585 (Long et al., 2015). We show that the amplitude of simulated terrestrial water mass over the
586 Upper Nile Basins varies substantially among various LSMs (see supplementary Fig. S15).
587 Most of these LSMs (GLDAS models: CLM, NOAH, VIC) do not include surface water or
588 groundwater storage (Scanlon et al., 2012). Although CLM (v.4.0 and 4.5) includes a simple
589 representation (i.e., shallow unconfined aquifer) of groundwater (Niu et al., 2007; Oleson et
590 al., 2008), it does not consider recharge from irrigation return flows. In addition, many of
591 these LSMs do not consider lakes and reservoirs and, most critically, LSMs are not
592 reconciled with in situ observations.

593

594 The combined measurement and leakage errors, $\sqrt{(bias^2 + leak^2)}$ (Swenson and Wahr,
595 2006) for *GRCTellus* ΔTWS based on CLM4.0 model for LVB and LKB are 7.2 cm and 6.6
596 cm respectively. These values, however, do not represent mass leakage from the lake to the
597 surrounding area within the basin itself. A sensitivity analysis of *GRCTellus* and GRGS

598 signals reveal that signal leakage occurs from lake to its surrounding basin area as well as
599 between basins. For instance, GRACE signal leakage into LKB from LVB, which is 3 times
600 larger in area than LKB, is 3.4 times bigger for both GRCTellus GRACE and GRGS
601 products. Furthermore, the analysis shows that leakage from Lake Victoria to LVB for
602 *GRCTellus* is substantially greater than GRGS product by a factor of ~2.6. In other words, 1
603 mm change in the level of Lake Victoria represents an equivalent change of 0.12 mm in
604 ΔTWS in LVB for *GRCTellus* compared to 0.32 mm for GRGS. Consequently, changes in
605 the amplitude of GRGS ΔTWS are much greater (~38 %) than *GRCTellus.* During the
606 observed reduction in ΔTWS (83 km^3) from 2003 to 2006, the computed volumetric
607 reduction for GRGS is found to be 69 km^3 whereas it is 31 km^3 for *GRCTellus*.
608
609 Another source of uncertainty that contributes toward ΔTWS anomalies in GRACE analysis
610 is the choice of simulated ΔSMS from various global-scale LSMs (e.g., Shamsudduha et al.,
611 2012; Scanlon et al., 2015). For example, the mean annual (2003−2012) amplitudes in
612 simulated ΔSMS in GLDAS LSMs (CLM, NOAH, VIC) vary substantially in LVB (3.5 cm,
613 10.2 cm, and 10.5 cm) and LKB (3.7 cm, 10.6 cm, and 7.7 cm) respectively. Due to an
614 absence of a dedicated monitoring network for soil moisture in the Upper Nile Basin, this
615 study like many other GRACE studies, is resigned to applying simulated ΔSMS from
616 multiple LSMs arguing that the use of an ensemble mean minimises the error associated with
617 ΔSMS (Rodell et al., 2009).
618
619 Computed contributions of ΔGWS to ΔTWS in the Upper Nile Basins are low (<10 %).
620 GRACE-derived estimates of ΔGWS from all three products (*GRCTellus*, GRGS and JPL-
621 Mascons) correlate very weakly with in situ ΔGWS in both LVB and LKB. One curious
622 observation in LVB during the unintended experiment (2003−2006) is that in situ ΔGWS

623 rises whereas in situ ΔSWS and simulated ΔSMS decline. The available evidence in
624 groundwater-level records (e.g., Entebbe, Uganda) suggests that rainfall-generated
625 groundwater recharge led to an increased in ΔGWS while dam releases exceeding the
626 "Agreed Curve" continued to reduce ΔSWS (Owor et al., 2011).
627
628 Uncertainties in the estimation of GRACE-derived ΔGWS remain in: (i) accurate
629 representation of the largest individual signal of in-situ ΔSWS in the disaggregation of
630 GRACE ΔTWS signal as it can limit the propagation of uncertainty in simulated ΔSMS, (ii)
631 simulated ΔSMS by GLDAS land surface models, (iii) the very limited spatial coverage in
632 piezometry to represent in situ ΔGWS, and (iv) applied S_y (3 % with range from 1 % to 6 %)
633 to convert in situ groundwater levels to ΔGWS. The lack of any strong correlation in
634 GRACE-derived ΔGWS and in situ ΔGWS time-series records indicates that the magnitude
635 of uncertainty is larger than the overall variability in ΔGWS in low-storage, low-
636 transmissivity weathered crystalline aquifers within the Upper Nile Basin. Furthermore,
637 statistically significant but negative correlations in both LVB and LKB arise from a positive
638 change in GRACE-derived ΔGWS when in situ ΔGWS is declining (e.g., 2003 to 2006 in
639 LVB; 2008 to 2010 in LKB). This inconsistency suggests that the 'true' GRACE ΔTWS
640 signal is weakened during processing and that the combined ΔSWS+ΔSMS signal is greater
641 than ΔTWS, mathematically resulting to a positive estimate of ΔGWS. In contrast to the
642 assertions of Nanteza et al. (2016) applying the *GRCTellus* CSR solution, we find that this
643 uncertainty prevents robust resolution of ΔGWS from GRACE ΔTWS in these complex
644 hydrogeological environments of East Africa. Despite substantial efforts to improve
645 groundwater-level monitoring and to collate existing groundwater-level records across
646 Africa, we recognise that understanding of in situ ΔGWS remains greatly constrained by
647 limitations in current observational networks and records. Since present uncertainties and

limitations identified in the Upper Nile Basin occur in many of the weathered hard-rock aquifer environments that underlie 40% of Sub-Saharan Africa (MacDonald et al., 2012), tracing of ΔGWS using GRACE in these areas is unlikely to be robust until these uncertainties and limitations are better constrained.

6. Conclusions

The analysis of a large, accurately recorded reduction of 1.2 m in the water level of Lake Victoria, equivalent to ΔSWS decline of 81 km^3 from 2004 to 2006 exposes substantial variability among commonly-used 5 gridded GRACE products (*GRCTellus* CSR, JPL, GFZ; GRGS; JPL-Mascons) to quantify the amplitude of changes in terrestrial water storage (ΔTWS). Around this event, we estimate an overall decline in 'in situ' or 'bottom-up' ΔTWS (i.e., in situ ΔSWS and ΔGWS; simulated ΔSMS) over the Lake Victoria Basin (LVB) of 83 km^3 from 2003 to 2006. This value compares favourably with JPL-Mascons GRACE ΔTWS (80 km^3), is underrepresented by GRGS GRACE ΔTWS (69 km^3), and is substantially underrepresented by the ensemble mean of *GRCTellus* GRACE ΔTWS (31 km^3). Attempts to better reconcile *GRCTellus* GRACE ΔTWS to bottom-up ΔTWS through scaling techniques are unable to represent adequately the observed amplitude in ΔTWS but highlight the uncertainty in the amplitude of gridded GRACE ΔTWS datasets generated by various processing strategies.

From 2003 to 2012, GRGS, JPL-Mascons and *GRCTellus* GRACE products trace well the phase in bottom-up ΔTWS in the Upper Nile Basin that comprises both the LVB and Lake Kyoga Basin (LKB). In the LVB for example, each explains 90 % (GRGS), 83 % (JPL-Mascons), and 75 % (*GRCTellus* ensemble mean of CSR, JPL and GFZ) of the variance, respectively, in bottom-up ΔTWS. The relative proportion of variability in bottom-up ΔTWS

673 (variance 120 cm^2 LVB, 24 cm^2 LKB) is explained by in situ ΔSWS (93 % LVB; 49 %
674 LKB), GLDAS ensemble mean ΔSMS (6 % LVB; 48 % LKB) and in situ ΔGWS (~1 %
675 LVB; 4 % LKB); these percentages are indicative and can vary as individual TWS
676 components are strongly correlated and the order of explanatory variables in regression
677 equation can affect the Analysis of Variance (ANOVA). In situ ΔGWS contributes minimally
678 to ΔTWS and is only moderately associated with GRACE ΔTWS (strongest correlation of
679 r=0.39, p-value <0.001). Resolution of ΔGWS from GRACE ΔTWS in the Upper Nile Basin
680 relies upon robust measures of ΔSWS and ΔSMS; the former is observed in situ whereas the
681 latter is limited by uncertainty in simulated ΔSMS, represented here and in many GRACE
682 studies by an ensemble mean of GLDAS LSMs. Mean annual amplitudes in observed ΔGWS
683 (2003–2012) from limited piezometry for the low-storage and low-transmissivity aquifers in
684 deeply weathered crystalline rocks that underlie the Upper Nile Basin are small (1.8 to 4.9 cm
685 for S_y= 0.03) and, given the current uncertainty in simulated ΔSMS, are beyond the limit of
686 what can be reliably quantified using current GRACE satellite products.
687
688 Our examination of a large, mass-storage change (2003 to 2006) observed in the Lake
689 Victoria Basin highlights substantial variability in the measurement of ΔTWS using different
690 gridded GRACE products. Although the phase in ΔTWS is generally well recorded by all
691 tested GRACE products, substantial differences exist in the amplitude of ΔTWS that also
692 influence the disaggregation of individual terrestrial stores (e.g., groundwater storage) and
693 estimation of trends in TWS and individual, disaggregated freshwater stores. We note that the
694 stronger filtering of the large-scale (~300 km) gravity signal associated with *GRCTellus*
695 results in greater signal leakage relative to GRGS and JPL-Mascons. As a result, greater
696 rescaling is required to resurrect signal amplitudes in *GRCTellus* relative to GRGS and JPL-
697 Mascons and these scaling factors depend upon uncertain and incomplete a priori knowledge

of terrestrial water stores derived from large-scale land-surface or hydrological models, which generally do not consider the existence of Lake Victoria, the second largest lake by area in the world.

Author contribution

RT conceived this study for which preliminary analyses were carried out by DJ and MS. MS and DJ have processed GRACE and all observational datasets and conducted statistical analyses and GIS mapping. LL conducted the analysis of spatial leakage and bias in GRACE signals. CT, RT and MO helped to establish, collate and analyse groundwater-level data; CT provided dam release data. MS and RT wrote the manuscript and LL, DJ, MO and CT commented on draft manuscripts.

Competing interests

The authors declare that they have no conflict of interest.

Acknowledgements

We kindly acknowledge NASA's MEaSUREs Program (http://grace.jpl.nasa.gov) for the freely available gridded *GRCTellus* and JPL-MASCON GRACE data and French National Centre for Space Studies (CNES) for GRGS GRACE data. NASA's Precipitation Processing Centre and NASA's Hydrological Sciences Laboratory and the Goddard Earth Sciences Data and Information Services Centre (GES DISC) are duly acknowledged for TRMM rainfall and soil moisture data from GLDAS Land Surface Models. We kindly acknowledge the Directorate of Water Resources Management in the Ministry of Water and Environment (Uganda) for the provision of piezometric and lake-level data. Support from the UK government's UPGro Programme, funded by the Natural Environment Research Council (NERC), Economic and Social Research Council (ESRC) and the Department For International Development (DFID) through the *GroFutures: Groundwater Futures in Sub-Saharan Africa* catalyst NE/L002043/1) and consortium (NE/M008932/1) grant awards, is gratefully acknowledged.

728 **References**

729

730 A, G., Wahr, J., and Zhong, S.: Computations of the viscoelastic response of a 3-D
731 compressible Earth to surface loading: an application to Glacial Isostatic Adjustment in
732 Antarctica and Canada, Geophys. J. Int., 192, 557-572, doi:10.1093/gji/ggs030, 2013.

733 Arendt, A. A., Luthcke, S. B., Gardner, A. S., O'Neel, S., Hill, D., Moholdt, G., and Abdalati,
734 W.: Analysis of a GRACE global mascon solution for Gulf of Alaska glaciers, Journal
735 of Glaciology, 59, 913-924, doi:10.3189/2013JoG12J197, 2013.

736 Awange, J. L., Sharifi, M. A., Ogonda, G., Wickert, J., Grafarend, E., and Omulo, M.: The
737 falling Lake Victoria water levels: GRACE, TRIMM and CHAMP satellite analysis of
738 the lake basin, Water Resources Management, 22, 775-796, 2008.

739 Awange, J. L., Anyah, R., Agola, N., Forootan, E., and Omondi, P.: Potential impacts of
740 climate and environmental change on the stored water of Lake Victoria Basin and
741 economic implications, Water Resour. Res., 49, 8160-8173, 2013.

742 Awange, J. L., Forootan, E., Kuhn, M., Kusche, J., and Heck, B.: Water storage changes and
743 climate variability within the Nile Basin between 2002 and 2011, Advances in Water
744 Resources, 73, 1-15, 2014.

745 Basalirwa, C. P. K.: Delineation of Uganda into climatological rainfall zones using the
746 method of Principle Component Analysis, International Journal of Climatology, 15,
747 1161-1177, 1995.

748 Becker, M., LLovel, W., Cazenave, A., Güntner, A., and Crétaux, J.-F.: Recent hydrological
749 behaviour of the East African great lakes region inferred from GRACE, satellite
750 altimetry and rainfall observations, Comptes Rendus Geoscience, 342, 223-233, 2010.

751 Biancale, R., Lemoine, J.-M., Balmino, G., Loyer, S., Bruisma, S., Perosanz, F., Marty, J.-C.,
752 and Gégout, P.: 3 Years of Geoid Variations from GRACE and LAGEOS Data at 10-
753 day Intervals from July 2002 to March 2005, CNES/GRGS, 2006.

754 Brown, E., and Sutcliffe, J. V.: The water balance of Lake Kyoga, Uganda, Hydrological
755 Sciences Journal, 58, 342-353, doi: 10.1080/02626667.2012.753148, 2013.

Bruinsma, S., Lemoine, J.-M., and Biancale, R.: CNES/GRGS 10-day gravity field models (release 2) and their evaluation Adv. Space Res., 45, 587-601, 10.1016/j.asr.2009.10.012, 2010.

Burgess, W. G., Shamsudduha, M., Taylor, R. G., Zahid, A., Ahmed, K. M., Mukherjee, A., Lapworth, D. J., and Bense, V. F.: Terrestrial water load and groundwater fluctuation in the Bengal Basin, Scientific Reports, 10.1038/s41598-017-04159-w, 2017.

Castellazzi, P., Martel, R., Galloway, D. L., Longuevergne, L., and Rivera, A.: Assessing Groundwater Depletion and Dynamics Using GRACE and InSAR: Potential and Limitations, Ground Water, doi:10.1111/gwat.12453, 2016.

Chen, J. L., Wilson, C. R., and Tapley, B. D.: The 2009 exceptional Amazon flood and interannual terrestrial water storage change observed by GRACE, Water Resour. Res., 46, W12526, 2010.

Dai, Y., Zeng, X., Dickinson, R. E., Baker, I., Bonan, G. B., Bosilovich, M. G., Denning, A. S., Dirmeyer, P. A., Houser, P. R., Niu, G., Oleson, K. W., Schlosser, C. A., and Yang, Z.-L.: The common land model (CLM), Bull. Am. Meteorol. Soc., 84, 1013-1023, 2003.

Ek, M. B., Mitchell, K. E., Lin, Y., Rogers, E., Grunmann, P., Koren, V., Gayno, G., and Tarpley, J. D.: Implementation of Noah land surface model advances in the National Centers for Environmental Prediction operational mesoscale Eta model, J. Geophys. Res., 108(D22), 8851, 10.1029/2002JD003296, 2003.

Famiglietti, J. S., Lo, M., Ho, S. L., Bethune, J., Anderson, K. J., Syed, T. H., Swenson, S. C., Linage, C. R. d., and Rodell, M.: Satellites measure recent rates of groundwater depletion in California's Central Valley, Geophys. Res. Lett., 38, L03403, 10.1029/2010GL046442, 2011.

Frappart, F., Ramillien, G., and Famiglietti, J. S.: Water balance of the Arctic drainage system using GRACE gravimetry products, International Journal of Remote Sensing, 32, 431-453, doi:10.1080/01431160903474954, 2011.

Güntner, A.: Improvement of Global Hydrological Models Using GRACE Data, Surveys in Geophysics, 29, 375-397, 2008.

785 Hoogeveen, J., Faurès, J.-M., Peiser, L., Burke, J., and Giesen, N. v. d.: GlobWat – a global
786 water balance model to assess water use in irrigated agriculture, Hydrol. Earth Syst.
787 Sci., 19, 3829-3844, 2015.

788 Hu, L., and Jiao, J. J.: Calibration of a large-scale groundwater flow model using GRACE
789 data: a case study in the Qaidam Basin, China, Hydrogeol. J., 23, 1305-1317, 2015.

790 Huffman, G. J., Adler, R. F., Bolvin, D. T., Gu, G., Nelkin, E. J., Bowman, K. P., Hong, Y.,
791 Stocker, E. F., and Wolff, D. B.: The TRMM multi-satellite precipitation analysis:
792 quasi-global, multi-year, combined-sensor precipitation estimates at fine scale, J.
793 Hydrometeorol., 8 (1), 38-55, 2007.

794 Humphrey, V., Gudmundsson, L., and Seneviratne, S. I.: Assessing Global Water Storage
795 Variability from GRACE: Trends, Seasonal Cycle, Subseasonal Anomalies and
796 Extremes, Surveys in Geophysics, 37, 357-395, doi:10.1007/s10712-016-9367-1, 2016.

797 Indeje, M., Semazzi, F. H. M., and Ogallo, L. J.: ENSO signals in East African rainfall
798 seasons, International Journal of Climatology, 20, 19-46, 2000.

799 Jacob, T., Wahr, J., Pfeffer, W. T., and Swenson, S.: Recent contributions of glaciers and ice
800 caps to sea level rise, Nature, 482, 514-518, 2012.

801 Jiang, D., Wang, J., Huang, Y., Zhou, K., Ding, X., and Fu, J.: The Review of GRACE Data
802 Applications in Terrestrial Hydrology Monitoring, Advances in Meteorology, Article
803 ID 725131, 2014.

804 Khandu, Forootan, E., Schumacher, M., Awange, J. L., and Schmied, H. M.: Exploring the
805 influence ofprecipitation extremes and humanwater use on total water storage
806 (TWS)changes in the Ganges-Brahmaputra-Meghna River Basin, Water Resour. Res.,
807 52, 2240-2258, doi:10.1002/2015WR018113, 2016.

808 Kim, H., Yeh, P. J.-F., Oki, T., and Kanae, S.: Role of rivers in the seasonal variations of
809 terrestrial water storage over global basins, Geophys. Res. Lett., 36, L17402,
810 doi:10.1029/2009GL039006, 2009.

811 Kizza, M., Westerberg, I., Rodhe, A., and Ntale, H.: Estimating areal rainfall over Lake
812 Victoria and its basin using ground-based and satellite data, Journal of Hydrology, 464-
813 465, 401-411, 2012.

814 Krishnamurthy, K. V., and Ibrahim, A. M.: Hydrometeorological Studies of Lakes Victoria,
815 Kyoga, and Albert, in: Unintended Lakes: Their Problems and Environmental Effects,

edited by: Ackermann, W. C., White, G. F., Worthington, E. B., and Ivens, J. L., American Geophysical Union, Washington D.C., 2013.

Kusche, J., Eicker, A., Forootan, E., Springer, A., and Longuevergne, L.: Mapping probabilities of extreme continental water storage changes from space gravimetry, Geophys. Res. Lett., 43, 8026-8034, doi:10.1002/2016GL069538, 2016.

Landerer, F. W., and Swenson, S. C.: Accuracy of scaled GRACE terrestrial water storage estimates, Water Resour. Res., 48, W04531, 2012.

Leblanc, M. J., Tregoning, P., Ramillien, G., Tweed, S. O., and Fakes, A.: Basin-scale, integrated observations of the early 21st century multiyear drought in southeast Australia, Water Resour. Res., 45, W04408, doi:10.1029/2008WR007333, 2009.

Lehner, B., Verdin, K., and Jarvis, A.: HydroSHEDS technical documentation, World Wildlife Fund, Washington D.C., 2006.

Lehner, B., Verdin, K., and Jarvis, A.: New global hydrography derived from spaceborne elevation data, Eos, Transactions American Geophysical Union, 89, 93-94, 2008.

Lemoine, J.-M., Bruisma, S., Loyer, S., Biancale, R., Marty, J.-C., Perosanz, F., and Balmino, G.: Temporal gravity field models inferred from GRACE data, Adv. Space Res., 39, 1620-1629, doi: 10.1016/j.asr.2007.03.062, 2007.

Liang, X., Xie, Z., and Huang, M.: A new parameterization for surface and groundwater interactions and its impact on water budgets with the variable infiltration capacity (VIC) land surface model, J. Geophys. Res., 108(D16), 8613, 10.1029/2002JD003090, 2003.

Long, D., Longuevergne, L., and Scanlon, B. R.: Global analysis of approaches for deriving total waterstorage changes from GRACE satellites, Water Resour. Res., 51, 2574–2594, doi:10.1002/2014WR016853, 2015.

Long, D., Chen, X., Scanlon, B. R., Wada, Y., Hong, Y., Singh, V. P., Chen, Y., Wang, C., Han, Z., and Yang, W.: Have GRACE satellites overestimated groundwater depletion in the Northwest India Aquifer?, Nature Scientific Reports, 6, 24398, doi:10.1038/srep24398, 2016.

Longuevergne, L., Scanlon, B. R., and Wilson, C. R.: GRACE hydrological estimates for small basins: evaluating processing approaches on the High Plains Aquifer, USA, Water Resour. Res., 46, W11517, 2010.

847 Longuevergne, L., Wilson, C. R., Scanlon, B. R., and Crétaux, J. F.: GRACE water storage
848 estimates for the Middle East and other regions with significant reservoir and lake
849 storage, Hydrol. Earth Syst. Sci., 17, 4817-4830, doi:10.5194/hess-17-4817-2013,
850 2013.

851 MacDonald, A. M., Bonsor, H. C., Dochartaigh, B. E. O., and Taylor, R. G.: Quantitative
852 maps of groundwater resources in Africa, Environ. Res. Lett., 7, doi:10.1088/1748-
853 9326/1087/1082/024009, 2012.

854 Nanteza, J., de Linage, C. R., Thomas, B. F., and Famiglietti, J. S.: Monitoring groundwater
855 storage changes in complex basement aquifers: An evaluation of the GRACE satellites
856 over East Africa, Water Resour. Res., 52, doi:10.1002/2016WR018846, 2016.

857 Nicholson, S. E., Yin, X., and Ba, M. B.: On the feasibility of using a lake water balance
858 model to infer rainfall: an example from Lake Victoria, Hydrological Science Journal,
859 45, 75-95, 2000.

860 Niu, G.-Y., Yang, Z.-L., Dickinson, R. E., Gulden, L. E., and Su, H.: Development of a
861 simple groundwater model for use in climate models and evaluation with Gravity
862 Recovery and Climate Experiment data, J. Geophys. Res., 112, D07103,
863 doi:10.1029/2006JD007522, 2007.

864 Oleson, K. W., Niu, G.-Y., Yang, Z.-L., Lawrence, D. M., Thornton, P. E., Lawrence, P. J.,
865 Stockli, R., Dickinson, R. E., Bonan, G. B., Levis, S., Dai, A., and Qian, T.:
866 Improvements to the Community Land Model and their impact on the hydrological
867 cycle, J. Geophys. Res., 113, G01021, doi:10.1029/2007JG000563, 2008.

868 Owor, M., Taylor, R. G., Tindimugaya, C., and Mwesigwa, D.: Rainfall intensity and
869 groundwater recharge: empirical evidence from the Upper Nile Basin, Environmental
870 Research Letters, 1-6, 2009.

871 Owor, M.: Groundwater - surface water interactions on deeply weathered surfaces of low
872 relief in the Upper Nile Basin of Uganda, Ph.D., Geography, University College
873 London, London, 271 pp., 2010.

874 Owor, M., Taylor, R. G., Mukwaya, C., and Tindimugaya, C.: Groundwater/surface-water
875 interactions on deeply weathered surfaces of low relief: evidence from Lakes Victoria
876 and Kyoga, Uganda, Hydrogeol. J., 19, 1403-1420, 2011.

877 Ramillien, G., Famiglietti, J. S., and Wahr, J.: Detection of Continental Hydrology and
878 Glaciology Signals from GRACE: A Review, Surv. Geophys., 29, 361-374, 2008.

879 Rodell, M., and Famiglietti, J. S.: Terrestrial Water Storage Variations over Illinois: Analysis
880 of Observations and Implications for GRACE, Wat. Resour. Res., 37, 1327-1340, 2001.

881 Rodell, M., Houser, P. R., Jambor, U., Gottschalck, J., Mitchell, K., Meng, C.-J., Arsenault,
882 K., Cosgrove, B., Radakovich, J., Bosilovich, M., Entin, J. K., Walker, J. P., Lohmann,
883 D., and Toll, D.: The Global Land Data Assimilation System, Bull. Am. Meteorol. Soc.,
884 85, 381-394, 2004.

885 Rodell, M., Velicogna, I., and Famiglietti, J. S.: Satellite-based estimates of groundwater
886 depletion in India, Nature, 460, 999-1003, doi:10.1038/nature08238, 2009.

887 Rowlands, D. D., Luthcke, S. B., McCarthy, J. J., Klosko, S. M., Chinn, D. S., Lemoine, F.
888 G., Boy, J.-P., and Sabaka, T. J.: Global mass fluxsolutions from GRACE: A
889 comparison of parameter estimation strategies-Mass concentrations versus stokes
890 coefficients, J. Geophys. Res., 115, B01403, doi:10.1029/2009JB006546, 2010.

891 Scanlon, B. R., Longuevergne, L., and Long, D.: Ground referencing GRACE satellite
892 estimates of groundwater storage changes in the California Central Valley, USA, Water
893 Resour. Res., 48, W04520, 2012.

894 Scanlon, B. R., Zhang, Z., Reedy, R. C., Pool, D. R., Save, H., Long, D., Chen, J., Wolock,
895 D. M., Conway, B. D., and Winester, D.: Hydrologic implications of GRACE satellite
896 data in the Colorado River Basin, Water Resour. Res., 51, 9891-9903,
897 doi:10.1002/2015WR018090, 2015.

898 Sene, K. J., and Plinston, D. T.: A review and update of the hydrology of Lake Victoria in
899 East Africa, Hydrological Sciences Journal, 39, 47-63, 1994.

900 Shamsudduha, M., Taylor, R. G., and Longuevergne, L.: Monitoring groundwater storage
901 changes in the highly seasonal humid tropics: validation of GRACE measurements in
902 the Bengal Basin, Water Resour. Res., 48, W02508, doi:10.1029/2011WR010993,
903 2012.

904 Strassberg, G., Scanlon, B. R., and Rodell, M.: Comparison of seasonal terrestrial water
905 storage variations from GRACE with groundwater-level measurements from the High
906 Plains Aquifer (USA), Geophys. Res.Lett., 34, L14402, 10.1029/2007GL030139, 2007.

907 Sun, A. Y., Green, R., Rodell, M., and Swenson, S.: Inferring aquifer storage parameters
908 using satellite and in situ measurements: Estimation under uncertainty, Geophys. Res.
909 Lett., 37, L10401, 10.1029/2010GL043231, 2010.

910 Sutcliffe, J. V., and Petersen, G.: Lake Victoria: derivation of a corrected natural water level
911 series, Hydrological Sciences Journal, 52, 1316-1321, 2007.

912 Swenson, S., and Wahr, J.: Post-processing removal of correlated errors in GRACE data,
913 Geophys. Res. Lett., 33, L08402, doi:10.1029/2005GL025285, 2006.

914 Tapley, B., Flechtner, F., Watkins, M., and Bettadpur, S.: GRACE mission: status and
915 prospects, 2015 GRACE Science Team Meeting, Austin, Texas, September 20-22,
916 2015, 2015.

917 Tapley, B. D., Bettadpur, S., Ries, J. C., Thompson, P. F., and Watkins, M. M.: GRACE
918 measurements of mass variability in the Earth system, Science, 305, 503-505, 2004.

919 Taylor, R., Tindimugaya, C., Barker, J., MacDonald, D., and Kulabako, R.: Convergent radial
920 tracing of viral and solute transport in gneiss saprolite, Ground Water, 48, 284-294,
921 2010.

922 Taylor, R. G., and Howard, K. W. F.: A tectonic geomorphic model of the hydrogeology of
923 deeply weathered crystalline rock: evidence from Uganda, Hydrogeol. J., 8, 279-294,
924 2000.

925 Taylor, R. G., Todd, M. C., Kongola, L., Maurice, L., Nahozya, E., Sanga, H., and
926 MacDonald, A. M.: Evidence of the dependence of groundwater resources on extreme
927 rainfall in East Africa, Nature Climate Change, 3, 374-378, doi:10.1038/nclimate1731,
928 2013.

929 UNEP: Adaptation to Climate-change Induced Water Stress in the Nile Basin: A
930 Vulnerability Assessment Report, Division of Early Warning and Assessment
931 (DEWA). United Nations Environment Programme (UNEP), Nairobi, Kenya, 2013.

932 Vishwakarma, B. D., Devaraju, B., and Sneeuw, N.: Minimizing the effects of filtering on
933 catchment scale GRACE solutions, Water Resour. Res., 52, 5868-5890,
934 doi:10.1002/2016WR018960, 2016.

935 Vouillamoz, J. M., Lawson, F. M. A., Yalo, N., and Descloitres, M.: The use of magnetic
936 resonance sounding for quantifying specific yield and transmissivity in hard rock
937 aquifers: The example of Benin, Journal of Applied Geophysics, 107, 16-24, 2014.

938 Wahr, J., Swenson, S., Zlotnicki, V., and Velicogna, I.: Time-variable gravity from GRACE:
939 First results, Geophys. Res. Lett., 31, L11501, doi:10.1029/2004GL019779, 2004.

940 Wahr, J., Swenson, S., and Velicogna, I.: Accuracy of GRACE mass estimates, Geophys.
941 Res. Lett., 33, L06401, doi:10.1029/2005GL025305, 2006.

942 Wang, L., Davis, J. L., Hill, E. M., and Tamisiea, M. E.: Stochasticfiltering for determining
943 gravityvariations for decade-long timeseries of GRACE gravity, J. Geophys.Res. Solid
944 Earth, 121, 2915-2931, doi:10.1002/2015JB012650, 2016.

945 Watkins, M. M., Wiese, D. N., Yuan, D.-N., Boening, C., and Landerer, F. W.: Improved
946 methods for observing Earth's time variable mass distribution with GRACE using
947 spherical cap mascons, J. Geophys. Res. Solid Earth, 120, 2648–2671,
948 doi:10.1002/2014JB011547, 2015.

949 Wiese, D. N., Yuan, D.-N., Boening, C., Landerer, F. W., and Watkins, M. M.: JPL GRACE
950 Mascon Ocean, Ice, and Hydrology Equivalent Water Height JPL RL05M.1. Ver. 1,
951 PO.DAAC, CA, USA, 2015.

952 Wiese, D. N., Landerer, F. W., and Watkins, M. M.: Quantifying and reducing leakage errors
953 in the JPL RL05M GRACE mascon solution, Water Resour. Res., 52, 7490-7502,
954 doi:10.1002/2016WR019344, 2016.

955 Xie, H., Longuevergne, L., Ringler, C., and Scanlon, B. R.: Calibration and evaluation of a
956 semi-distributed watershed model of Sub-Saharan Africa using GRACE data, Hydrol.
957 Earth Syst. Sci., 16, 3083-3099, 2012.

958 Yin, X., and Nicholson, S. E.: The water balance of Lake Victoria, Hydrol. Sci. J., 43, 789-
959 811, 1998.

960

961

962 **Figure Captions**

963

964 **Figure 1.** Map of the study area encompassing the Lake Victoria Basin (LVB) and Lake
965 Kyoga Basin (LKB), and location of the in situ monitoring stations. The Upper Nile Basin is
966 marked by a rectangle (red) within the entire Nile River Basin shown as a shaded relief index
967 map. Piezometric monitoring (red circles) and lake-level gauging (dark blue squares) stations
968 are shown on the map.

969

970 **Figure 2.** Observed daily total dam releases (blue line) and the agreed curve (red line) at the
971 outlet of Lake Victoria in Jinja from November 2007 to July 2009 (Owor et al., 2011).

972

973 **Figure 3.** Mean annual rainfall for the period of 2003–2012 derived from TRMM satellite
974 observations. Greater annual rainfall is observed over much of the Lake Victoria and
975 northeastern corner of the Lake Victoria Basin.

976

977 **Figure 4.** Seasonal pattern (monthly mean from January 2003 to December 2012) of TRMM-
978 derived monthly rainfall, various GRACE-derived ΔTWS signals [GRCTellus=ensemble
979 mean of CSR, JPL and GFZ; GRGS and JPL-Mascons (MSCN) products], the bottom-up
980 TWS; GLDAS LSMs ensemble mean ΔSMS, in situ ΔSWS and borehole-derived estimate of
981 ΔGWS over the Lake Victoria Basin.

982

983 **Figure 5.** Monthly time-series datasets for the Lake Victoria Basin (LVB) from January 2003
984 to December 2012: (a) *GRCTellus* GRACE-derived ΔTWS (ensemble mean of CSR, GFZ,
985 and JPL), GRGS and JPL-Mascons ΔTWS time-series data; (b) GLDAS-derived ΔSMS
986 (individual signals as well as an ensemble mean of NOAH, CLM, and VIC); (c) lake-level-
987 derived ΔSWS; and (d) borehole-derived ΔGWS time-series data. Note that monthly rainfall
988 records derived from TRMM satellite are plotted on panel (d) where the dashed horizontal
989 line represents the mean monthly rainfall for the period of January 2003 to December 2012.

990

991 **Figure 6.** Monthly time-series datasets for the Lake Kyoga Basin (LKB) from January 2003
992 to December 2012: (a) *GRCTellus* GRACE-derived ΔTWS (ensemble mean of CSR, GFZ,
993 and JPL), GRGS and JPL-Mascons ΔTWS time-series data; (b) GLDAS-derived ΔSMS
994 (individual signals as well as an ensemble mean of NOAH, CLM, and VIC); (c) lake-level-

995 derived ΔSWS; and (d) borehole-derived ΔGWS time-series data. Note that monthly rainfall
996 records derived from TRMM satellite are plotted on panel (d) where the dashed horizontal
997 line represents the mean monthly rainfall for the period of January 2003 to December 2012.
998
999 **Figure 7.** Comparison among time-series records of ΔTWS from *GRCTellus* (ensemble mean
1000 of CSR, GFZ, and JPL), GRGS and JPL-Mascons GRACE products and bottom-up ΔTWS
1001 for the Lake Victoria Basin (LVB) (a), and Lake Kyoga Basin (LKB) (b) for the period of
1002 January 2003 to December 2012. The vertical grey lines represent monthly rainfall anomalies
1003 in LVB and LKB.
1004
1005 **Figure 8.** Estimates of in situ ΔGWS and GRACE-derived ΔGWS time-series records
1006 (January 2003 to December 2012) in LVB show a substantial variations among themselves.
1007 An ensemble mean ΔSMS (GLDAS 3 LSMs: CLM, NOAH and VIC) and an unscaled ΔSWS
1008 are applied in the disaggregation of ΔGWS using *GRCTellus* GRACE (ensemble mean of
1009 CSR, GFZ, and JPL) and JPL-Mascons products.
1010
1011 **Figure 9.** Taylor diagram shows strength of statistical association, variability in amplitudes
1012 of time-series records and agreement among the reference data, bottom-up ΔTWS and
1013 *GRCTellus* GRACE-derived ΔTWS (ensemble mean of CSR, GFZ, and JPL, GRGS and JPL-
1014 Mascons ΔTWS time-series records), simulated ΔSMS (ensemble mean of NOAH, CLM and
1015 VIC), in situ ΔSWS, and in situ ΔGWS over the LVB. The solid arcs around the reference
1016 point (black square) indicate centred Root Mean Square (RMS) differences among bottom-up
1017 ΔTWS and other variables, and the dashed arcs from the origin of the diagram indicate
1018 variability in time-series records. Data for Lake Victoria Basin (LVB) are only shown in this
1019 diagram.
1020

1021 **Table 1.** Estimated areal extent (km^2) of the Lake Victoria Basin (LVB), Lake Kyoga Basin
1022 (LKB), Lake Victoria and Lake Kyoga.
1023

Basin/Lake	**This study** [*HydroSHEDS* database]	**UNEP (2013)**	**Awange et al. (2014)**
Lake Victoria Basin	256 100	184 000	258 000
Lake Victoria	67 220	68 800	-
Lake Kyoga Basin	79 270	75 000	75 000
Lake Kyoga	2 730	1 720	-

1024
1025
1026
1027

1028 **Table 2.** Details of groundwater and lake level monitoring stations located in Lake Victoria
1029 Basin and Lake Kyoga Basin.
1030

Monitoring Station	Basin	Parameter	Longitude	Latitude	Depth (m bgl)
Apac	LKB	Groundwater level	32.50	1.99	15.0
Pallisa	LKB	Groundwater level	33.69	1.20	46.2
Soroti	LKB	Groundwater level	33.63	1.69	66.0
Bugondo	LKB	Lake level	33.20	0.45	-
Entebbe	LVB	Groundwater level	32.47	0.04	48.0
Rakai	LVB	Groundwater level	31.40	–0.69	53.0
Nkokonjeru	LVB	Groundwater level	32.91	0.24	30.0
Jinja	LVB	Lake level	33.23	1.59	-

1031

1032 **Table 3.** Linear trends (cm yr^{-1}) in GRACE ΔTWS and bottom-up ΔTWS in Lake Victoria
1033 Basin and Lake Kyoga Basin over various time periods (statistically significant trends, *p*
1034 values <0.05 are marked by an asterisk).

Period	GRACE Ensemble	GRGS	JPL-Mascons	Bottom-up TWS
Lake Victoria Basin (LVB)				
2003–2006	–4.10*	–9.00*	–10.0*	–11.00*
2007–2012	–0.31	1.50*	2.70*	1.10*
2003–2012	0.04	0.58	1.00*	0.54
Lake Kyoga Basin (LKB)				
2003–2006	–2.10*	–4.60*	–3.50*	–2.80*
2007–2012	0.22	2.00*	1.50*	0.48
2003–2012	–0.01	0.54*	0.54*	–0.56*

1035

1036

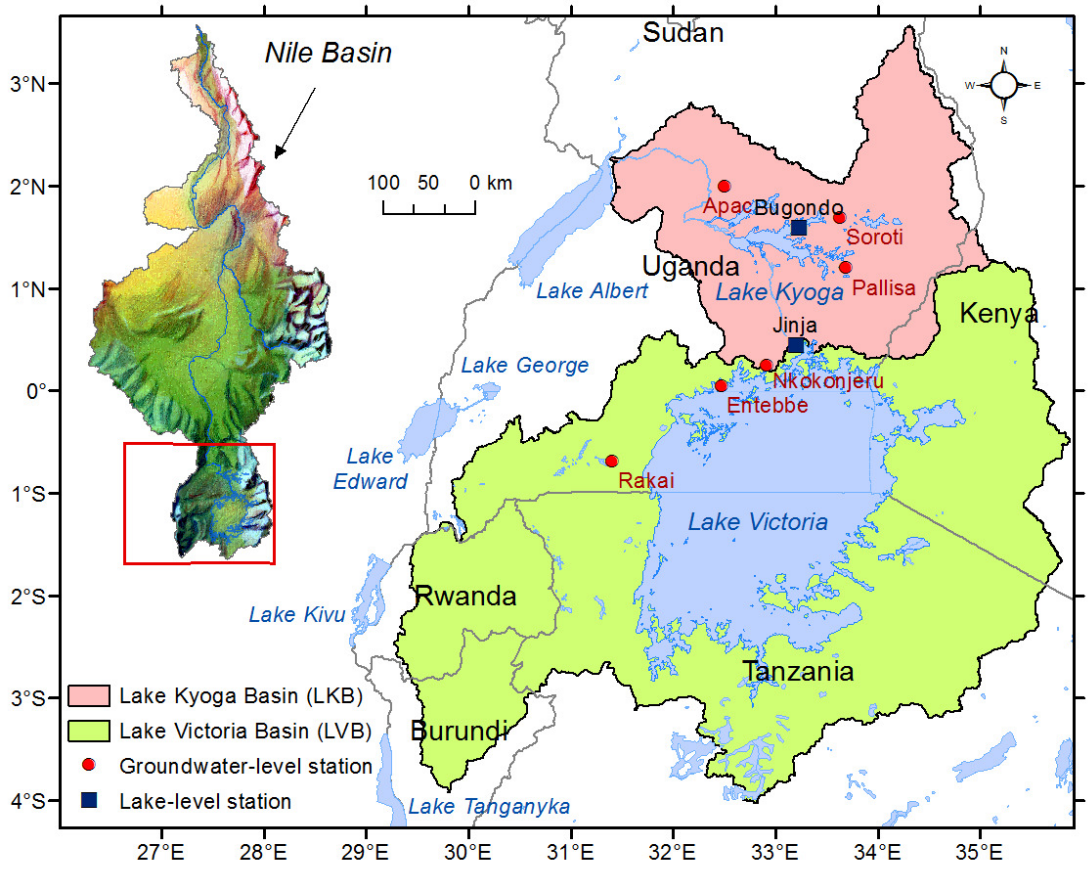

Figure 1. Map of the study area encompassing the Lake Victoria Basin (LVB) and Lake Kyoga Basin (LKB), and location of the in situ monitoring stations. The Upper Nile Basin is marked by a rectangle (red) within the entire Nile River Basin shown as a shaded relief index map. Piezometric monitoring (red circles) and lake-level gauging (dark blue squares) stations are shown on the map.

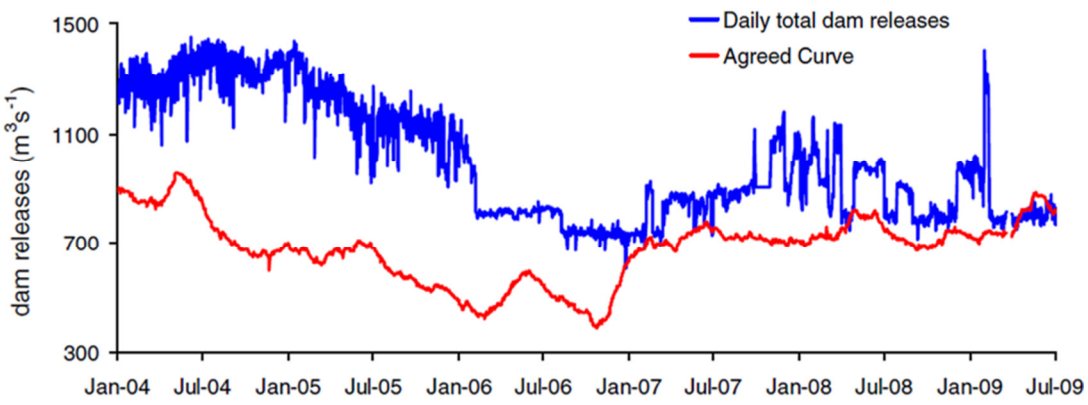

Figure 2. Observed daily total dam releases (blue line) and the agreed curve (red line) at the outlet of Lake Victoria in Jinja from November 2007 to July 2009 (Owor et al., 2011).

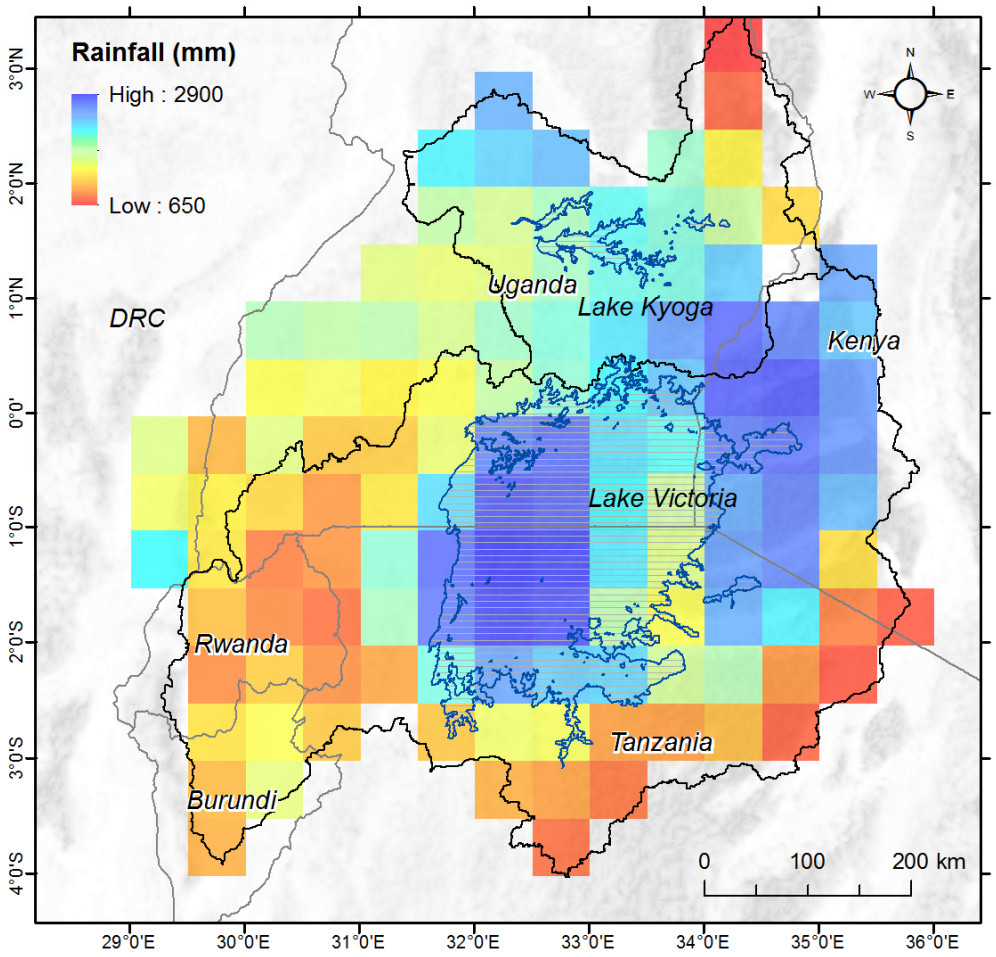

Figure 3. Mean annual rainfall for the period of 2003–2012 derived from TRMM satellite observations. Greater annual rainfall is observed over much of the Lake Victoria and northeastern corner of the Lake Victoria Basin.

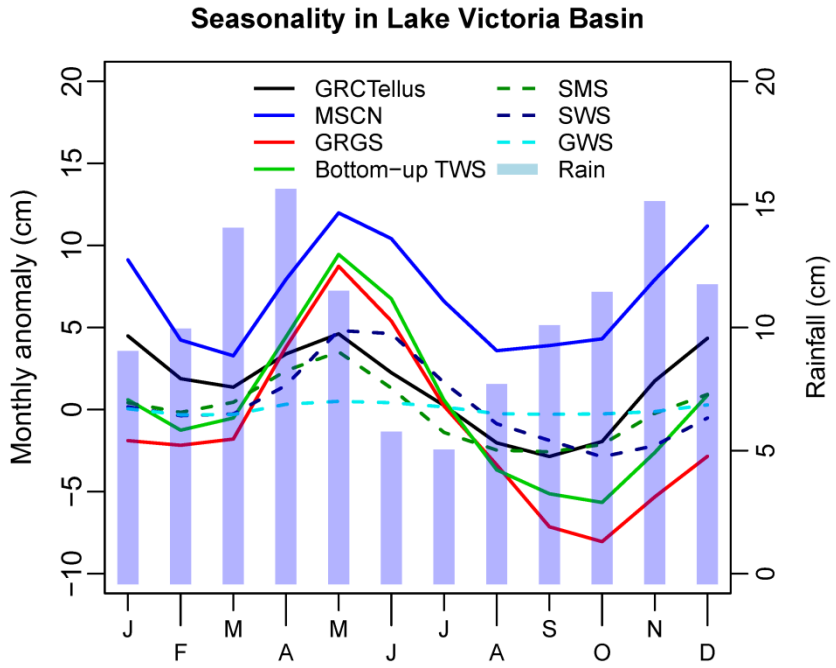

Figure 4. Seasonal pattern (monthly mean from January 2003 to December 2012) of TRMM-derived monthly rainfall, various GRACE-derived ΔTWS signals [GRCTellus=ensemble mean of CSR, JPL and GFZ; GRGS and JPL-Mascons (MSCN) products], the bottom-up TWS; GLDAS LSMs ensemble mean ΔSMS, in situ ΔSWS and borehole-derived estimate of ΔGWS over the Lake Victoria Basin.

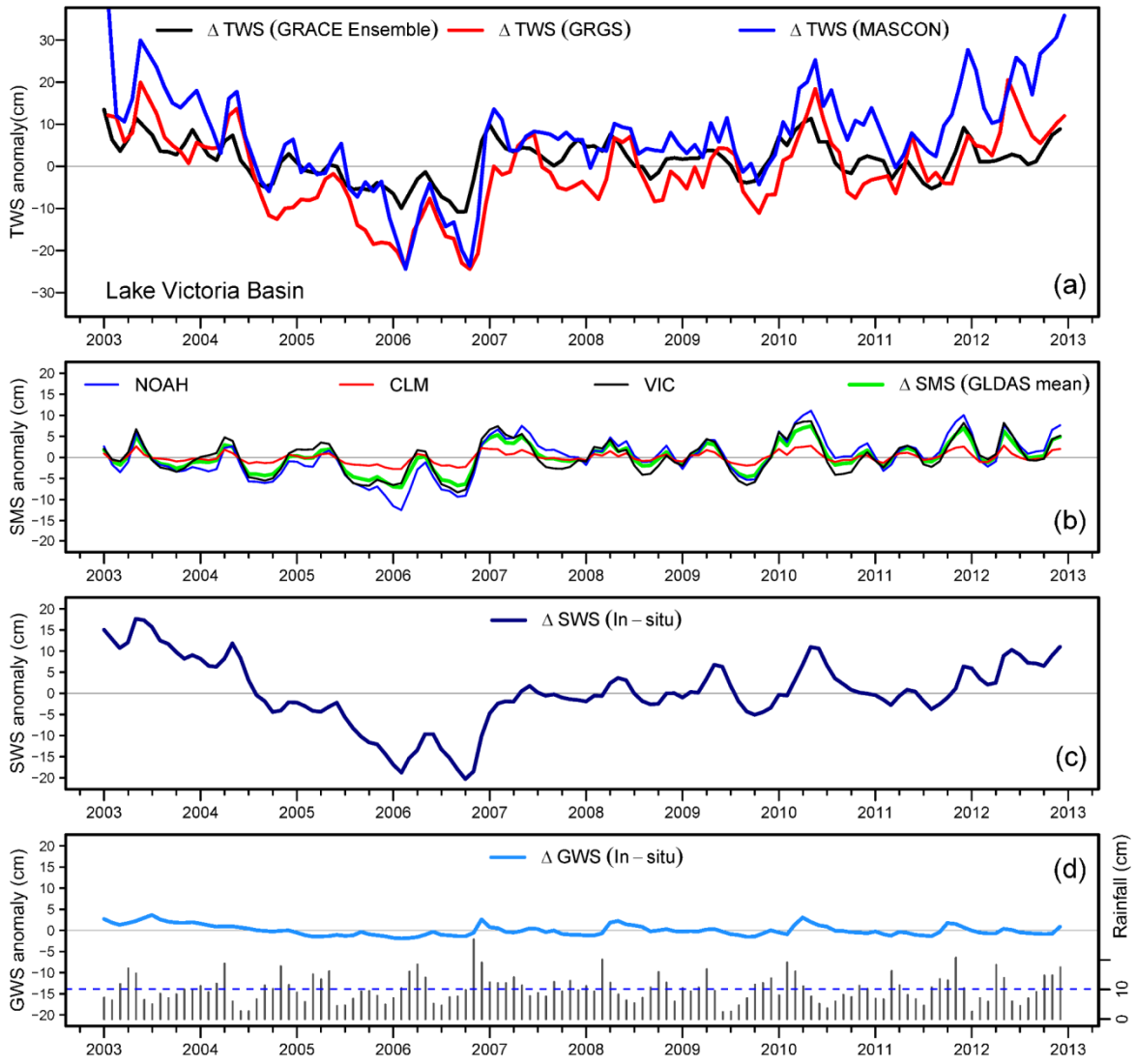

Figure 5. Monthly time-series datasets for the Lake Victoria Basin (LVB) from January 2003 to December 2012: (a) *GRCTellus* GRACE-derived ΔTWS (ensemble mean of CSR, GFZ, and JPL), GRGS and JPL-Mascons ΔTWS time-series data; (b) GLDAS-derived ΔSMS (individual signals as well as an ensemble mean of NOAH, CLM, and VIC); (c) lake-level-derived ΔSWS; and (d) borehole-derived ΔGWS time-series data. Note that monthly rainfall records derived from TRMM satellite are plotted on panel (d) where the dashed horizontal line represents the mean monthly rainfall for the period of January 2003 to December 2012.

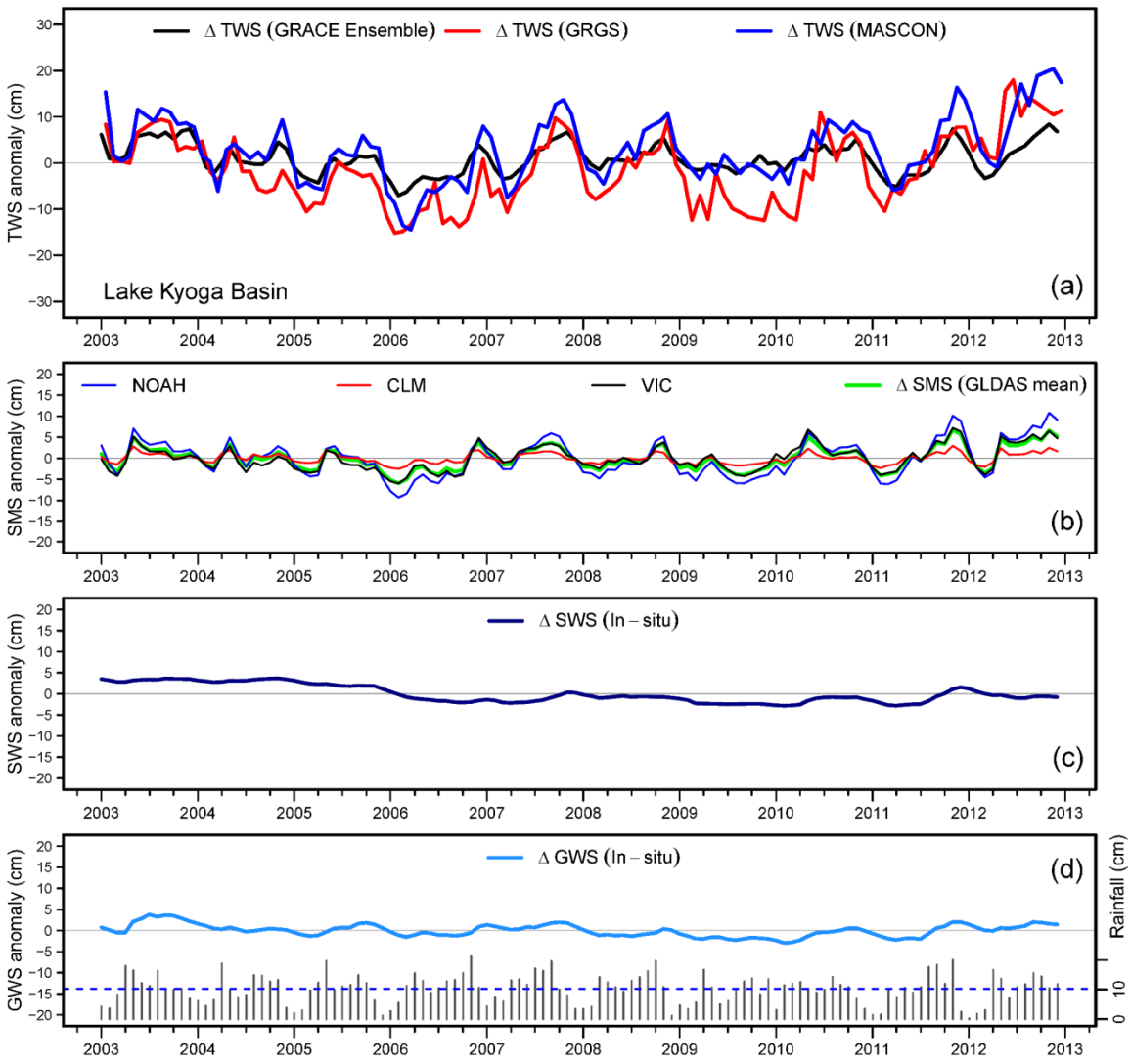

Figure 6. Monthly time-series datasets for the Lake Kyoga Basin (LKB) from January 2003 to December 2012: (a) *GRCTellus* GRACE-derived ΔTWS (ensemble mean of CSR, GFZ, and JPL), GRGS and JPL-Mascons ΔTWS time-series data; (b) GLDAS-derived ΔSMS (individual signals as well as an ensemble mean of NOAH, CLM, and VIC); (c) lake-level-derived ΔSWS; and (d) borehole-derived ΔGWS time-series data. Note that monthly rainfall records derived from TRMM satellite are plotted on panel (d) where the dashed horizontal line represents the mean monthly rainfall for the period of January 2003 to December 2012.

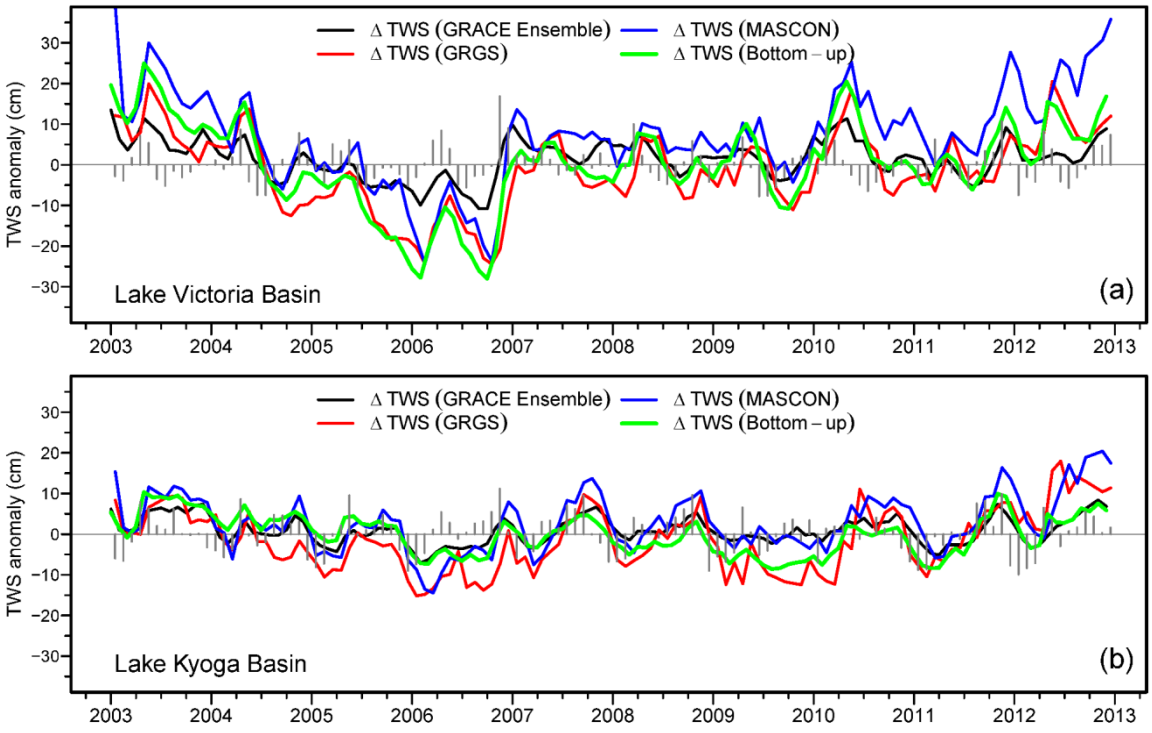

Figure 7. Comparison among time-series records of ΔTWS from *GRCTellus* (ensemble mean of CSR, GFZ, and JPL), GRGS and JPL-Mascons GRACE products and bottom-up ΔTWS for the Lake Victoria Basin (LVB) (a), and Lake Kyoga Basin (LKB) (b) for the period of January 2003 to December 2012. The vertical grey lines represent monthly rainfall anomalies in LVB and LKB.

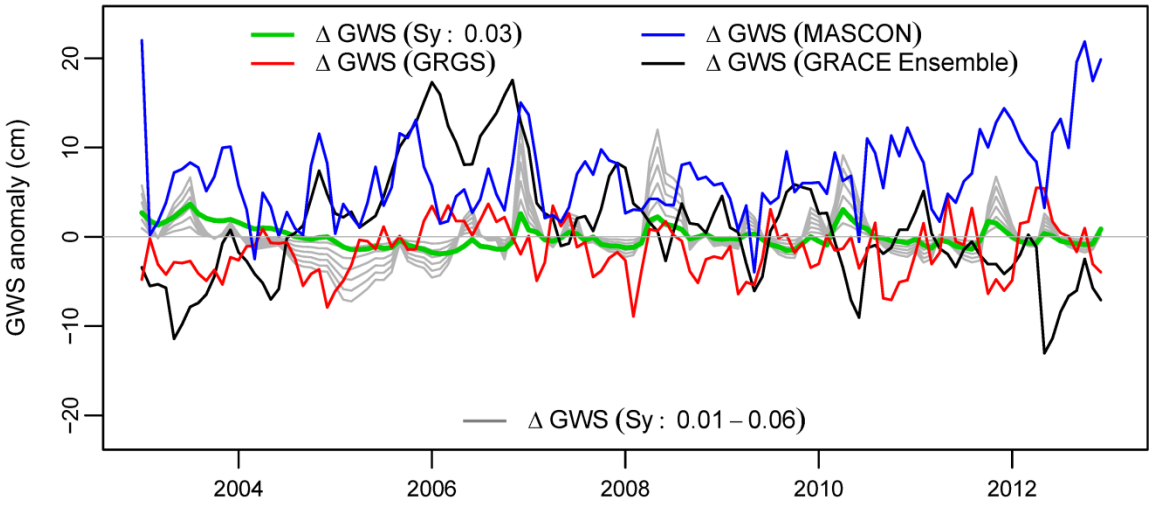

Figure 8. Estimates of in situ ΔGWS and GRACE-derived ΔGWS time-series records (January 2003 to December 2012) in LVB show a substantial variations among themselves. An ensemble mean ΔSMS (GLDAS 3 LSMs: CLM, NOAH and VIC) and an unscaled ΔSWS are applied in the disaggregation of ΔGWS using *GRCTellus* GRACE (ensemble mean of CSR, GFZ, and JPL)and JPL-Mascons products.

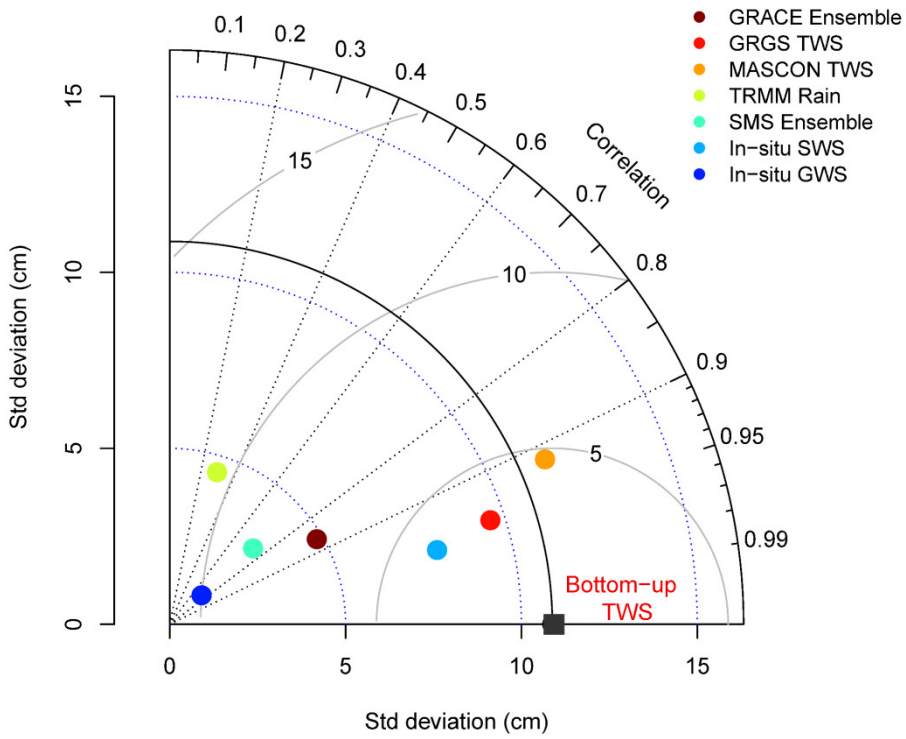

Figure 9. Taylor diagram shows strength of statistical association, variability in amplitudes of time-series records and agreement among the reference data, bottom-up ΔTWS and *GRCTellus* GRACE-derived ΔTWS (ensemble mean of CSR, GFZ, and JPL, GRGS and JPL-Mascons ΔTWS time-series records), simulated ΔSMS (ensemble mean of NOAH, CLM and VIC), in situ ΔSWS, and in situ ΔGWS over the LVB. The solid arcs around the reference point (black square) indicate centred Root Mean Square (RMS) differences among bottom-up ΔTWS and other variables, and the dashed arcs from the origin of the diagram indicate variability in time-series records. Data for Lake Victoria Basin (LVB) are only shown in this diagram.